INVESTIGATION ON STRUCTURAL DAMAGES OF RESIDENTAL RC BUILDINGS SUFFERED DUE TO KAHRAMANMARAŞ EARTHQUAKES

Editor

BETÜL ÜSTÜNER

BİDGE Yayınları

INVESTIGATION ON STRUCTURAL DAMAGES OF RESIDENTIAL RC BUILDINGS SUFFERED DUE TO KAHRAMANMARAŞ EARTHQUAKES

Authors: TAHA YASİN ALTIOK, CANSU BERİL ESER, BARIŞ SERİN, MEHMET ŞEVİK, MEHMET BAKIR BOZKURT, ALİ DEMİR

Editor: BETÜL ÜSTÜNER

ISBN: 978-625-372-784-0

1. Baskı

Sayfa Düzeni: Gözde YÜCEL

Yayınlama Tarihi: 25.06.2025

BİDGE Yayınları

Sertifika No: 71374

www.bidgeyayinlari.com.tr - bidgeyayinlari@gmail.com
Krc Bilişim Ticaret ve Organizasyon Ltd. Şti.
Güzeltepe Mahallesi Abidin Daver Sokak Sefer Apartmanı No: 7/9 Çankaya / Ankara

BİDGE Yayınları

CONTENTS

PREFACE

On February 6, 2023, a devastating seismic event began with an Mw 7.7 magnitude earthquake centered in Pazarcık, Kahramanmaraş, followed only a few hours later by a second major earthquake of Mw 7.6. This extraordinary sequence of earthquakes significantly affected 11 provinces in Türkiye, marking one of the most destructive natural disasters in the country's history. Numerous aftershocks followed, and thousands of buildings either completely collapsed or sustained severe damage. Tragically, tens of thousands of lives were lost, hundreds of thousands were injured, and the lives of millions were profoundly impacted.

This study presents a comprehensive engineering evaluation of the seismic events that led to this extensive devastation. The primary focus is on residential reinforced concrete buildings, which suffered the most severe damage in the affected areas. Structural deficiencies, irregularities, and the resulting damage are meticulously documented and analyzed. Furthermore, the seismic behavior of a five-story residential building that collapsed as a result of the earthquakes is assessed in detail using acceleration records from the nearest station, with analysis focusing on inter-story displacements, story drifts, accelerations, forces, and overall performance.

This book serves not only as a technical investigation for the engineering community but also as a critical resource for mitigating the impacts of similar disasters in the future. It has been prepared with the utmost care to support both academic research and practical applications in structural design and assessment.

I extend my sincere gratitude to all authors and contributors who played a role in bringing this important work to fruition. I hope this publication provides valuable insights and benefits to all its readers.

Editor

Dr. Betül Üstüner

Introduction

Earthquakes are one of the most destructive and deadly natural disasters that cannot be detected in advance. Turkey woke up at 04:17 on February 6, 2023, with an earthquake centered in Kahramanmaraş/Pazarcık with a magnitude of Mw 7.7. 11 minutes after the earthquake, which took place at a depth of 8.6 km, an aftershock occurred due to the first earthquake with a magnitude of Mw 6.6, centered in Gaziantep/Nurdağı and at a depth of 6.0 km. Approximately 9 hours later, before the effects of the previous earthquake had passed, the region was shaken again by an earthquake centered in Kahramanmaraş/Elbistan with a magnitude of Mw 7.6 at a depth of 7.0 km. Many structures that survived the destructiveness of the first earthquake could not withstand the second earthquake and collapsed. 14 days after these earthquakes, the fourth major earthquake with a magnitude of Mw 6.4 occurred at a depth of 21.73 km underground in Hatay Yayladağı, approximately 160 km away from the first earthquake. The earthquake deeply affected 11 cities. The total surface area of these cities is 108,812 km2 and covers 14% of the country's territory.

Tragically, more than 50,000 people lost their lives, and more than 100,000 people were injured. Thousands of structures were destroyed or severely damaged. The destroyed infrastructure and physical capital are estimated to be approximately 50 billion US dollars, which corresponds to approximately 6% of Turkey's Gross Domestic Product [1]. Immediately after the earthquake, an international call for help was made, and 266 international urban search and rescue (USAR) teams with more than 11,700 professional personnel were deployed for the first time in the world [2].

Turkey is located in the Alpine-Himalayan seismic zone, one of the most active earthquake regions in the world. There are three main tectonic elements in the country: Eastern Anatolian Fault Zone, North Anatolian Fault Zone and Aegean Graben systems. This results in a very complex tectonic system. Active fault zones and the geography in which they are located have caused many earthquakes throughout history, many people lost their lives, were injured, and many structures were damaged [3–6]. In Turkey, which has a very high seismic risk, 20 earthquakes with a magnitude above 7.0 have occurred since 1900 [7]. In the last 25 years in Turkey, earthquakes with magnitude 6 and above occurred in 1998 Adana (Mw 6.3), 1999 Izmit (Mw 7.6), 1999 Düzce (Mw 7.2), 2003 Bingöl (Mw 6.4), 2010 Kovancılar (Mw 6.1), 2011 Van (Mw 7.2), 2017 Manisa (Mw 6.6), 2020 Samos (Mw 6.6), 2020 Düzce (Mw 6.7), 2020 Elazığ/Sivrice (Mw 6.8), 2023 Kahramanmaraş/Pazarcık (Mw 7.7) and Kahramanmaraş/Elbistan (Mw7.6) [8].

The devastating earthquakes in the east of the country occurred with the rupture of a 450 km strike-slip fault on the Eastern Anatolian Fault Zone. The Eastern Anatolian Fault is an important fault that represents the boundary between the Arabian Plate and the Anatolian Plate and extends along the eastern part of the country. The tectonics of the fault are related to the approach of the Arabian plate to the Anatolian Plate. This situation causes earthquakes with both strike-slip and thrust components. The Eastern Anatolian Fault Zone was very active in the 19th century and created a series of earthquakes that started with the 1822 Antakya earthquake and ended with the 1866, 1872, 1874, 1875, 1893, 1905 Malatya earthquake, respectively. The fault zone, which had accumulated energy for a while, broke with the 2020 Elazığ earthquake and caused many people to lose their lives [9].

It is crucial to evaluate the destructive effects on buildings, reveal the tectonic situation of the region, determine the ground properties and determine the issues that negatively affect the earthquake performance of the existing building stock after earthquakes. Post-earthquake studies carried out by different disciplines are an integral part of modern disaster management. The studies carried out in this context are of great importance in determining earthquake and structural risks, revealing structural damages and developing earthquake-resistant building design principles. In the literature, there are many studies on field investigations for bridges, historical buildings, masonry structures, RC structures, industrial buildings, timber structures, and other structures after earthquakes [3,10–29]. After the Kahramanmaraş earthquakes, researchers went to the earthquake region and carried out their studies within the scope of different disciplines. Işık et al. (2023) [30] carried out studies on the widespread damage and collapse mechanisms of masonry structures in Adıyaman. In addition, the distribution of building damages was presented statistically based on the seismicity of the region and the spectral acceleration values of the Kahramanmaraş earthquakes. Ivanov and Chow (2023) discussed the structural damages and collapses that occurred in low and high RC structures in Adıyaman province. They attributed most of the damage to poor materials, poor workmanship, and failure to comply with earthquake-resistant construction techniques. Öztürk et al. (2023) [31] discussed the structural damages and their causes on school buildings after the earthquake. Response spectrum and elastic design spectrum were compared. The observations made were supported by performance-based analytical studies. Işık et al. (2023) [32] 27 investigated the effects of earthquakes on 27 different mosques and minarets. They determined that the damages occurring in these types of structures were commonly caused due to the fact that they were made by local foreman without any engineering services. Zengin and Aydin (2023) [33] investigated the relationship between material quality and destruction and structural damages in Kahramanmaraş/Elbistan. They performed core, Schmidt, and UPV tests. They found that many structures, including buildings constructed after 2000, did not have sufficient concrete compressive strength. Yıldız and Kına (2023) [34] examined the design and manufacturing mistakes on damaged and collapsed buildings in Malatya province. Akar et al. (2024) [9] examined the effects of the earthquake in Adıyaman/Gölbaşı after the earthquakes centered in

Kahramanmaraş. They carried out their studies on buildings with different structural systems. They determined that structural damages in the district center were generally caused by problems related to soil-structure interaction and revealed the importance of earthquake-soil-structure interaction. Avcil et al. (2024) [35] made observational evaluations of buildings with different structural systems in Kahramanmaraş and its districts. They found that masonry structures were generally damaged due to not receiving engineering services, that industrial buildings had insufficient connection details, and problems related to soil-structure interaction. Demir et al. (2024) [7] carried out geotechnical and structural investigations immediately after earthquakes. They stated that RC structures commonly have poor materials, poor workmanship, inappropriate reinforcement details, and inadequate construction techniques. İnce (2024) [36] found that earthquake damages of RC structures in Adıyaman were generally due to inappropriate material quality, structural design, and reinforcement details. Kocakaplan et al. (2024) [37] carried out field investigations as a team after the earthquakes and investigated structural and non-structural damages and causes of collapse in RC structures. They also made suggestions to reduce damages caused by earthquakes and prevent deaths. Kocaman et al. (2024) [38] examined the effects of Kahramanmaraş-centered earthquakes on the historical Malatya Yeni Mosque. Dynamic analyses were carried out using acceleration records from Malatya city center on the finite element model of the mosque, a part of which collapsed due to the earthquake. It has been reported that the analysis results are quite compatible with field observations and that structural damage generally occurs in the dome, minaret, columns, and arch system. Altunsu et al. (2024) [39] made damage observations on RC, steel, and masonry structures in Hatay province. They determined that common damages generally consist of stirrup insufficiency, corrosion, poor material, insufficient interlocking length, strong beam-weak column problems, and construction errors. In addition, they demonstrated with different visuals that short columns, soft floors, hammering effects, and design errors also cause damage. Kahya et al. (2024) [40] performed nonlinear finite element analyses on a historical masonry building example in Hatay and compared it with field observations. The analysis results were consistent with the observed damage patterns. Additionally, in the study, suggestions were made for the repair and strengthening of masonry buildings. Çelik et al. (2024) [41] investigated the structural, geotechnical, and architectural conditions and problems in heavily damaged mid-rise RC residential buildings. According to field observations, it has been determined that architectural design mistakes and poor ground properties cause permanent damage to structural systems, and buildings with tunnel formwork systems performed well.

Within the scope of this study, structural damages and destructions that occurred in RC residential buildings in Kahramanmaraş, Hatay, Adana, Gaziantep, and Osmaniye provinces due to Kahramanmaraş-centered earthquakes were deeply examined in terms of structural and earthquake engineering, based on field observations. Structural damages occurring in RC residential buildings have been examined in detail under three main headings: mistakes in the design phase, mistakes in the application phase, and material properties. Additionally, response spectra were obtained using earthquake records from Adıyaman, Diyarbakır, Malatya, Kilis and Şanlıurfa provinces. Earthquake demands were evaluated by comparing them with the elastic design spectrum obtained according to the principles of the Turkish Building Earthquake Regulation-2018 (TBEC-2018) In this context, the earthquakes centered in Kahramanmaraş/Pazarcık (Mw 7.7), Gaziantep/Nurdağı (Mw 6.6), Kahramanmaraş/Elbistan (Mw 7.6) and Hatay/Yayladağı (Mw 6.4), which had the most destructive effects, were taken as a basis. In addition, the population characteristics of the earthquake area, comprehensive data on the existing building stock, and damage assessment results were discussed in detail from different perspectives. Finally, based on the analysis of structural damages and response spectrum in line with the findings, various suggestions have been presented to reduce the destructive effects of possible earthquakes in the future. Furthermore, the seismic behavior of a five-story residential building that collapsed during the earthquake was analyzed using nonlinear time-history analyses based on acceleration records obtained from the nearest station. The factors contributing to the building’s collapse, including story displacements, story accelerations, story drifts, and performance analysis results, were reported.

Strong Ground Motion

The max. ground accelerations (PGA), maximum ground velocities (PGV), and maximum displacements (PGD) read from the earthquakes centered in Kahramanmaraş/Pazarcık, Gaziantep/Nurdağı, Kahramanmaraş/Elbistan Hatay/Yayladağı are given in Table 1, respectively.

Table 1 Magnitudes of Kahramanmaraş earthquakes and PGA, PGV, PGD values

Date	Place (Earthquake ID)	Latitude (0)	Longitude (0)	Depth km	Magnitude M_w	PGA cm/sn^2 (g)	PGV cm/sn	PGD cm
06.02.2023 04:17	Pazarcık K.maraş (543428)	37.288	37.043	8.6	7.7	2178.71 **(2.22 g)**	186.78	132.68
06.02.2023 04:28	Nurdağı Gaziantep (543431)	37.304	36.920	6.2	6.6	454.15 **(0.46 g)**	44.60	214.37
06.02.2023 13:24	Elbistan K.maraş (543593)	38.089	37.239	7.0	7.6	635.45 **(0.65 g)**	170.79	90.99
20.02.2023 20:04	Yayladağı Hatay (551067)	36.037	36.021	21.73	6.4	775.40 **(0.79 g)**	75.79	37.52

In this section, response spectra were obtained using some of the peak ground acceleration records of the provinces of Adana, Adıyaman, Diyarbakır, Gaziantep, Hatay, Malatya, Kahramanmaraş, Kilis, Şanlıurfa and Osmaniye, which were most affected by the Kahramanmaraş and Hatay earthquakes. These response spectra were compared with the elastic design spectrum determined according to the principles of TBEC-2018 [42] and information about each province was presented separately under subheadings.

Adana

The peak ground acceleration value in Adana during the Kahramanmaraş and Hatay earthquakes was read as 0.41g in the east-west direction by the accelerometer placed in Saimbeyli district number 0131 in the Elbistan earthquake. The largest ground accelerations (PGA) and the largest response spectrum accelerations of Saimbeyli district, as well as Çukurova and Yumurtalık districts, are given in Table 2, and the comparison of the response spectrum with the elastic design spectrum is given in Figure 1. As shown in Figure 1, it is seen that the spectral accelerations of station 0118 in Adana Çukurova exceed the elastic design spectrum accelerations in regions where the period is approximately greater than 1.5 seconds, and the spectral accelerations of station 0131 in Saimbeyli exceed the elastic design spectrum accelerations in regions where the period is close to 0.5 seconds.

Table 2 Peak ground acceleration and response spectrum values for Adana

City	District	Sta. No	Earthquake	max PGA (g)			max S_{ae} (g)			$(V_s)_{30}$ m/s	Soil class
				EW	NS	UD	EW	NS	UD		
Adana	Çukurova	0118	Pazarcık	0.05	0.04	0.02	0.118	0.125	0.068	946	ZB
			Nurdağı	0.01	0.01	0.01	0.050	0.034	0.023		
			Elbistan	0.03	0.02	0.02	0.073	0.114	0.071		
			Yayladağı	-	-	-	-	-	-		
	Yumurtalık	0120	Pazarcık	0.11	0.12	**0.11**	0.392	0.287	**0.313**	439	ZC
			Nurdağı	0.05	0.05	0.02	0.148	0.143	0.063		
			Elbistan	0.02	0.03	0.02	0.074	0.049	0.064		
			Yayladağı	0.03	0.02	0.01	0.093	0.073	0.036		
	Saimbeyli	0131	Pazarcık	0.16	0.16	0.05	0.646	0.646	0.170	-	ZD
			Nurdağı	0.06	0.06	0.02	0.266	0.273	0.057		
			Elbistan	**0.41**	**0.34**	0.09	**1.574**	**1.991**	0.259		
			Yayladağı	0.00	0.00	0.00	0.015	0.016	0.004		

Figure 1 Response spectrum and elastic design spectrum acquired in stations 0118, 0120, and 0131 located in Adana during the earthquakes

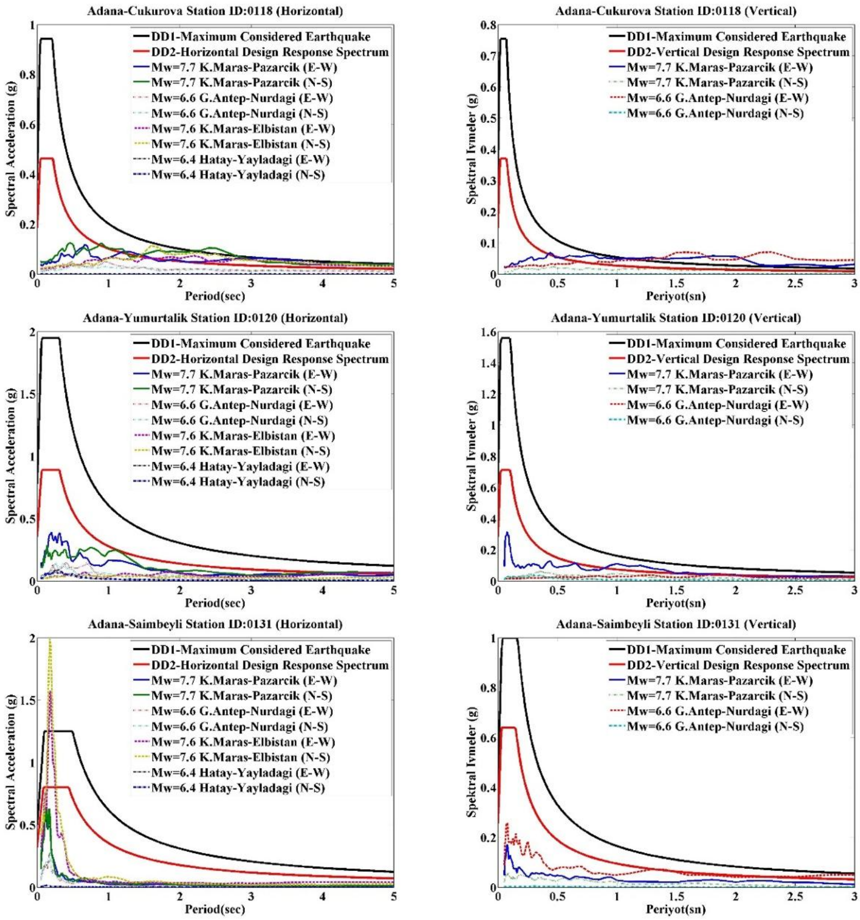

Adıyaman

The peak ground acceleration value in Adıyaman during the Kahramanmaraş and Hatay earthquakes was read as 0.90g in the north-south direction by the accelerometer placed in the Central district numbered 0201 in the Pazarcık earthquake. The largest ground accelerations (PGA) and the largest response spectrum accelerations of the city center and Tut districts are given in Table 3, and the comparison of the response spectrum with the elastic design spectrum is given in Figure 2. According to Figure 2, the spectral accelerations of station 0201 in Adıyaman Center exceed the elastic design spectrum accelerations in regions where the period is close to 0.5 seconds, and the spectral accelerations of station 0213 in Tut exceed the elastic design spectrum accelerations in regions where the period is greater than approximately 1.8 seconds.

Table 3 Peak ground acceleration and response spectrum values for Adıyaman

City	District	Sta. No	Earthquake	max PGA (g)			max S_{ae} (g)			$(V_s)_{30}$	Soil class
				EW	NS	UD	EW	NS	UD	m/s	
Adıyaman	Merkez	0201	Pazarcık	0.48	0.90	0.33	1.149	1.156	0.655	391	ZC
			Nurdağı	-	-	-	-	-	-		
			Elbistan	-	-	-	-	-	-		
			Yayladağı	0.01	0.01	0.00	0.022	0.022	0.010		
	Tut	0213	Pazarcık	0.25	0.18	0.30	0.784	0.672	0.708	-	ZD
			Nurdağı	-	-	-	-	-	-		
			Elbistan	0.12	0.13	0.07	0.517	0.471	0.222		
			Yayladağı	-	-	-	-	-	-		

Figure 2 Response spectrum and elastic design spectrum acquired from stations 0201 and 0213 located in Adıyaman during the earthquakes

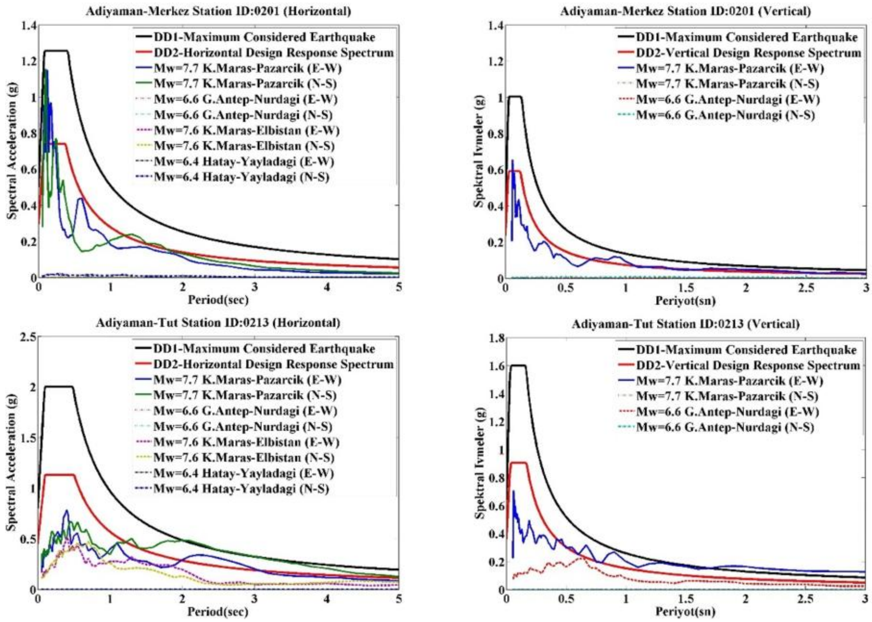

Diyarbakır

The peak ground acceleration value in Diyarbakır during the Kahramanmaraş and Hatay earthquakes was read as 0.12g in the north-south direction by the accelerometer placed in Ergani district number 2104 in the Pazarcık earthquake. The largest ground accelerations (PGA) and the largest response spectrum accelerations of Bağlar and Ergani districts are given in Table 4, and the comparison of the response spectrum with the elastic design spectrum is given in Figure 3. As shown in Figure 3, except for a few local regions in Diyarbakır province, the spectral accelerations caused by the earthquake are generally below the elastic design spectrum accelerations defined in TBEC-2018.

Table 4 Peak ground acceleration and response spectrum values for Diyarbakır

City	District	Sta. No	Earthquake	max PGA (g)			max S_{ae} (g)			$(V_s)_{30}$ m/s	Soil class
				EW	NS	UD	EW	NS	UD		
Diyarbakır	Bağlar	2101	Pazarcık	0.08	0.07	0.03	0.214	0.209	0.127	519	ZC
			Nurdağı	0.01	0.01	0.00	0.027	0.021	0.009		
			Elbistan	0.03	0.02	0.01	0.076	0.081	0.055		
			Yayladağı	-	-	-	-	-	-		
	Ergani	2104	Pazarcık	0.07	0.12	0.08	0.268	0.215	0.139	-	ZD
			Nurdağı	0.00	0.00	0.00	0.010	0.013	0.010		
			Elbistan	0.03	0.02	0.02	0.064	0.082	0.065		
			Yayladağı	-	-	-	-	-	-		

Figure 3 Response spectrum and elastic design spectrum acquired from stations 2101 and 2104 located in Diyarbakır during the earthquakes

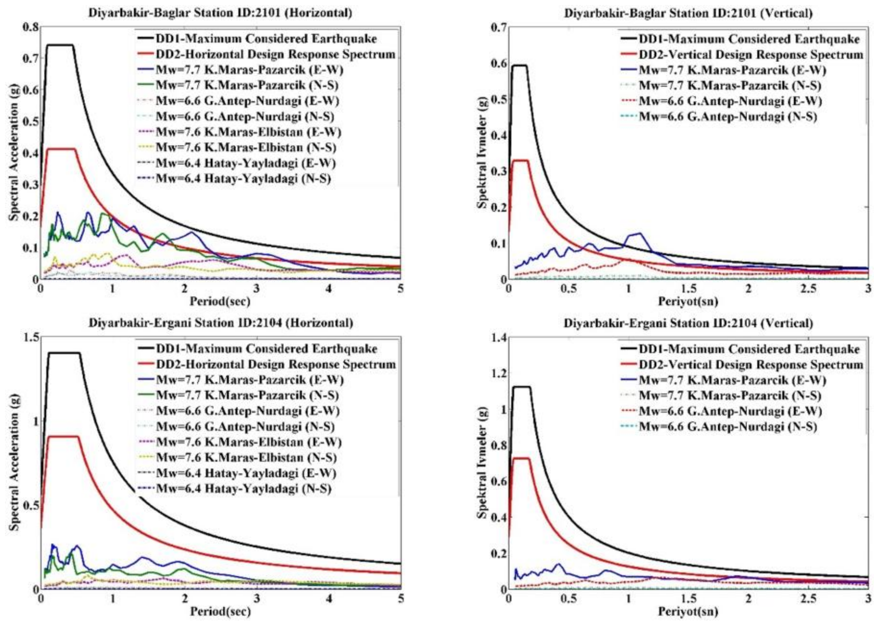

Gaziantep

The peak ground acceleration value in Gaziantep during these earthquakes was read as 0.72g in the east-west direction by the accelerometer placed in İslahiye district number 2718 in the Pazarcık earthquake. The largest ground accelerations (PGA) and the largest response spectrum accelerations of Islahiye and Nurdağı districts are given in Table 5, and the comparison of the response spectrum with the elastic design spectrum is given in Figure 4. According to Figure 4, it is seen that the spectral accelerations of stations 2712 and 2718 in Gaziantep exceed the elastic design spectrum accelerations defined in TBEC-2018 in the region corresponding to many periods.

Table 5 Peak ground acceleration and response spectrum values for Gaziantep

City	District	Sta. No	Earthquake	max PGA (g)			max S_{ae} (g)			$(V_s)_{30}$	Soil class
				EW	NS	UD	EW	NS	UD	m/s	
Gaziantep	İslahiye	2708	Pazarcık	-	-	-	-	-	-	523	ZC
			Nurdağı	0.32	0.38	0.22	1.145	1.142	0.652		
			Elbistan	-	-	-	-	-	-		
			Yayladağı	0.03	0.04	0.02	0.151	0.156	0.053		
	Nurdağı	2712	Pazarcık	0.57	0.61	0.35	1.787	1.846	1.008	-	ZD
			Nurdağı	0.46	0.35	0.37	1.056	1.328	0.784		
			Elbistan	-	-	-	-	-	-		
			Yayladağı	-	-	-	-	-	-		
	İslahiye	2718	Pazarcık	0.72	0.66	0.60	2.081	1.697	1.244	-	ZD
			Nurdağı	0.24	0.33	0.14	1.239	0.796	0.402		
			Elbistan	0.04	0.05	0.02	0.156	0.151	0.082		
			Yayladağı	0.02	0.03	0.02	0.085	0.081	0.060		

Figure 4 Response spectrum and elastic design spectrum acquired from stations 2708, 2712, and 2718 located in Gaziantep during the earthquakes

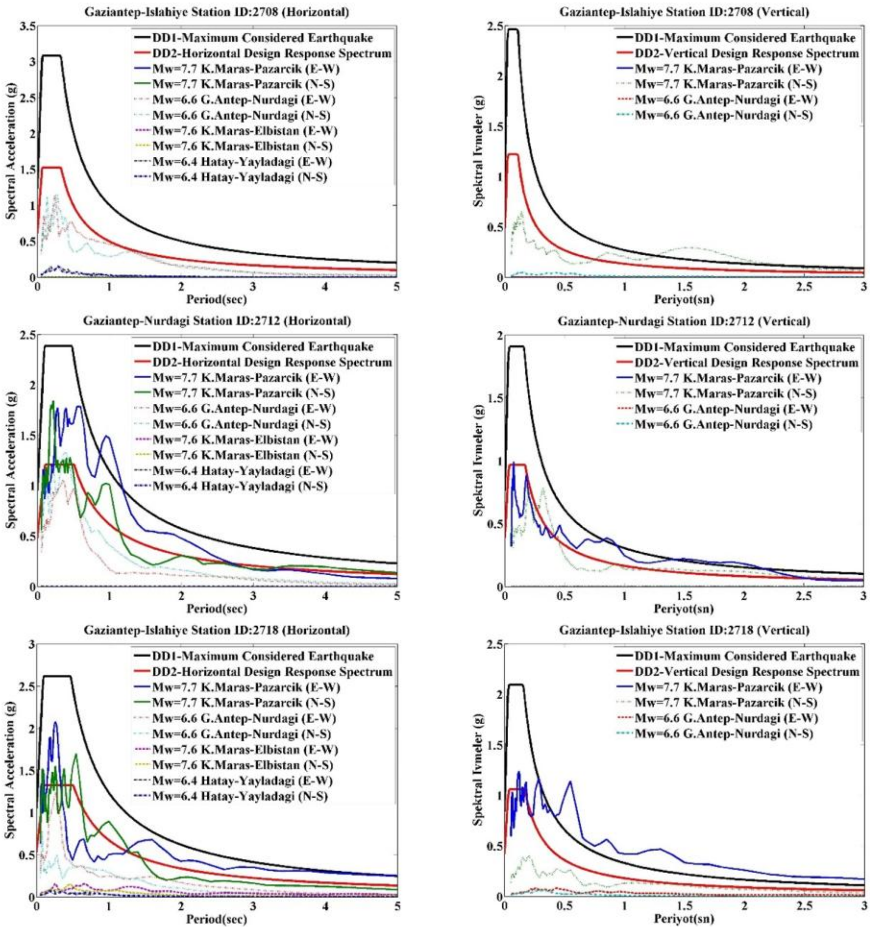

Hatay

The peak ground acceleration value in Hatay during these earthquakes was read as 1.40 g in the east-west direction by the accelerometer placed in Arsuz district number 3135 in the Pazarcık earthquake. The largest ground accelerations (PGA) and the largest response spectrum accelerations of Arsuz, Antakya, and Defne districts are given in Table 6, and the comparison of the response spectrum with the elastic design spectrum is given in Figure 5. As indicated in Figure 5, it is seen that the spectral accelerations of stations 3125, 3126, 3129, and 3135 in Hatay exceed the elastic design spectrum accelerations defined in TBEC-2018.

Table 6 Peak ground acceleration and response spectrum values for Hatay

City	District	Sta. No	Earthquake	max PGA (g)			max S_{ae} (g)			$(V_s)_{30}$ m/s	Soil class
				EW	NS	UD	EW	NS	UD		
Hatay	Antakya	3125	Pazarcık	0.84	1.14	1.17	2.458	2.109	3.145	448	ZC
			Nurdağı	0.39	0.25	0.12	0.756	1.579	0.286		
			Elbistan	0.03	0.02	0.02	0.073	0.069	0.056		
			Yayladağı	0.79	0.78	0.47	2.546	2.808	1.635		
	Antakya	3126	Pazarcık	1.23	1.05	1.09	2.566	5.156	3.225	350	ZD
			Nurdağı	0.21	0.32	0.13	0.997	0.684	0.415		
			Elbistan	-	-	-	-	-	-		
			Yayladağı	-	-	-	-	-	-		
	Defne	3129	Pazarcık	1.38	1.23	0.84	4.642	5.314	2.700	447	ZC
			Nurdağı	0.16	0.24	0.06	0.709	0.572	0.182		
			Elbistan	0.02	0.03	0.01	0.097	0.098	0.039		
			Yayladağı	-	-	-	-	-	-		
	Arsuz	3135	Pazarcık	0.76	1.40	0.60	2.998	1.923	2.298	460	ZC
			Nurdağı	0.05	0.05	0.03	0.118	0.112	0.070		
			Elbistan	0.02	0.02	0.01	0.046	0.053	0.038		
			Yayladağı	0.36	0.35	0.21	1.372	1.270	1.079		

Figure 5 Response spectrum and elastic design spectrum acquired from stations 3125, 3126, 3129, and 3125 located in Hatay during the earthquakes

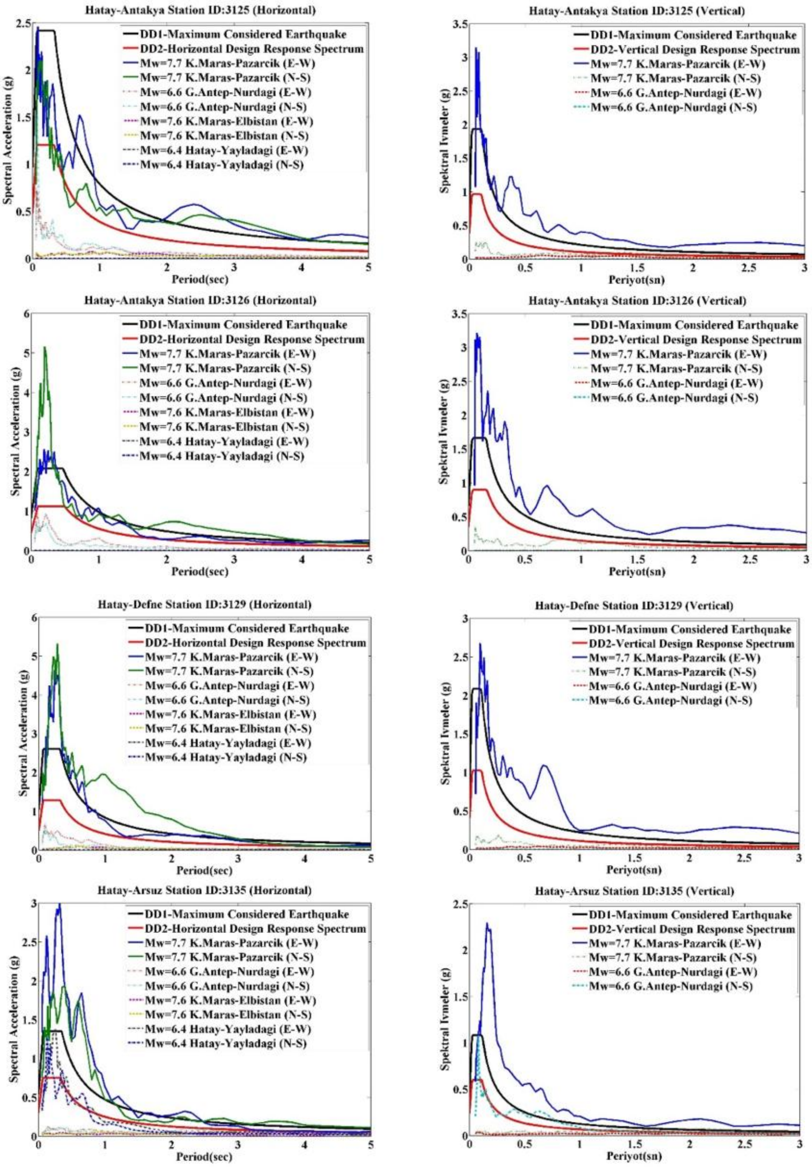

Malatya

The peak ground acceleration value in Malatya during these earthquakes was read as 0.48g in the east-west direction by the accelerometer placed in Akçadağ district number 4406 in the Elbistan earthquake. The largest ground accelerations (PGA) and the largest response spectrum accelerations of Akçadağ, Kale, and Pütürge districts are given in Table 7, and the comparison of the response spectrum with the elastic design spectrum is given in Figure 6. When the data received from station 4406 in Malatya is examined according to Figure 6, it can be seen that the spectral accelerations exceed the elastic design spectrum accelerations defined in TBEC-2018 in the region corresponding to many periods.

Table 7 Peak ground acceleration and response spectrum values for Malatya

City	District	Sta. No	Earthquake	max PGA (g)			max S_{ae} (g)			$(V_s)_{30}$ m/s	Soil class
				EW	NS	UD	EW	NS	UD		
Malatya	Pütürge	4404	Pazarcık	0.14	0.14	0.10	0.375	0.506	0.277	1380	ZB
			Nurdağı	0.00	0.01	0.00	0.019	0.013	0.012		
			Elbistan	0.05	0.05	0.04	0.156	0.150	0.128		
			Yayladağı	0.00	0.00	0.00	0.005	0.005	0.003		
	Akçadağ	4406	Pazarcık	0.11	0.13	0.05	0.323	0.237	0.158	815	ZB
			Nurdağı	0.01	0.01	0.01	0.046	0.051	0.024		
			Elbistan	0.48	0.42	0.33	1.526	1.372	1.005		
			Yayladağı	0.00	0.00	0.00	0.005	0.004	0.003		
	Kale	4414	Pazarcık	0.11	0.17	0.05	0.321	0.207	0.169	-	ZD
			Nurdağı	-	-	-	-	-	-		
			Elbistan	0.08	0.06	0.04	0.278	0.245	0.122		
			Yayladağı	0.00	0.00	0.00	0.008	0.005	0.002		

Figure 6 Response spectrum and elastic design spectrum acquired from stations 4404, 4406, and 4414 located in Malatya during the earthquakes

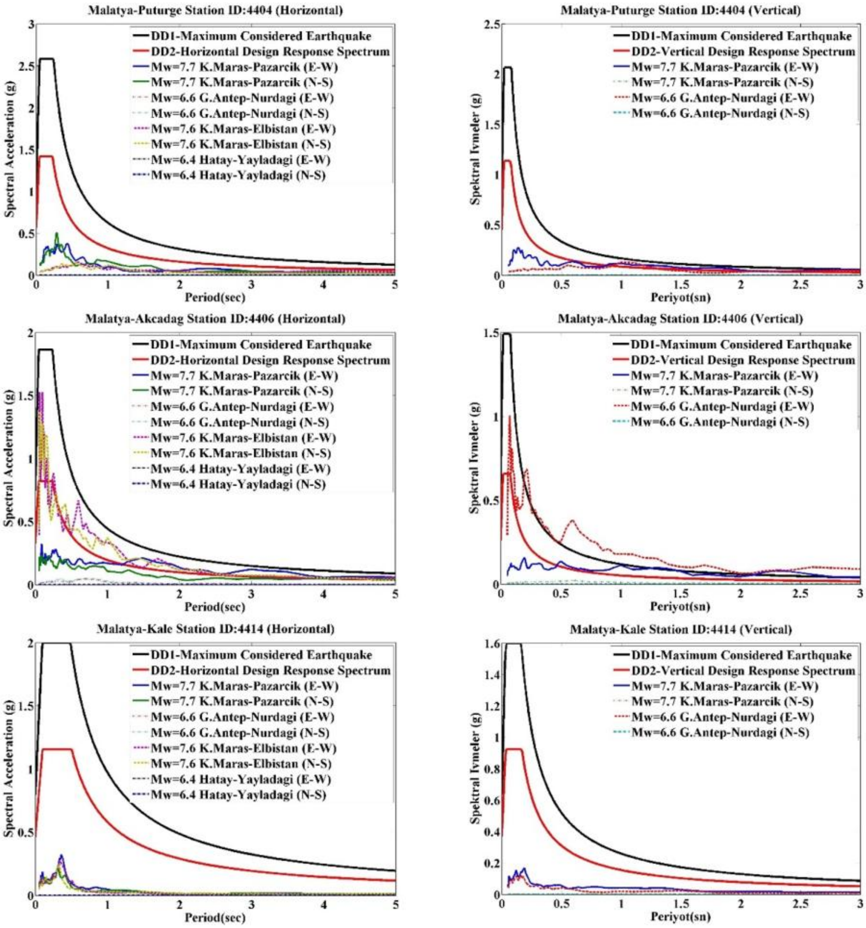

Kahramanmaraş

The peak ground acceleration value in Kahramanmaraş, which is the epicenter of two of these earthquakes, was read as 2.21g in the north-south direction by the accelerometer placed in Pazarcık district number 4614 in the Pazarcık earthquake. This value is the peak acceleration value in these four earthquakes. The largest ground accelerations (PGA) and the largest response spectral accelerations of Dulkadiroğlu, Göksun, Pazarcık, and Türkoğlu districts are given in Table 8, and the comparison of the response spectrum with the elastic design spectrum is given in Figure 7. According to Figure 7, when the data obtained from Kahramanmaraş's stations 4612, 4614, 4616, and 4625 reported above are examined, the spectral accelerations in the region corresponding to many periods exceed the elastic design spectrum accelerations defined in TBEC-2018.

Table 8 Peak ground acceleration and response spectrum values for Kahramanmaraş

City	District	Sta. No	Earthquake	max PGA (g)			max S_{ae} (g)			$(V_s)_{30}$ m/s	Soil class
				EW	NS	UD	EW	NS	UD		
Kahramanmaraş	Göksun	4612	Pazarcık	0.14	0.12	0.06	0.569	0.468	0.223	246	ZD
			Nurdağı	0.05	0.10	0.03	0.298	0.288	0.139		
			Elbistan	0.65	0.53	0.50	1.465	1.380	1.223		
			Yayladağı	0.01	0.01	0.00	0.042	0.054	0.018		
	Pazarcık	4614	Pazarcık	**2.21**	**2.22**	**1.99**	**5.862**	**7.487**	**5.775**	541	ZC
			Nurdağı	0.10	0.11	0.04	0.476	0.414	0.149		
			Elbistan	0.16	0.21	0.09	0.675	0.655	0.364		
			Yayladağı	0.01	0.01	0.00	0.021	0.026	0.011		
	Türkoğlu	4616	Pazarcık	0.67	0.51	0.41	1.270	2.507	1.612	390	ZC
			Nurdağı	0.25	0.27	0.17	0.762	1.006	0.747		
			Elbistan	0.06	0.05	0.03	0.212	0.216	0.098		
			Yayladağı	0.02	0.01	0.00	0.038	0.060	0.014		
	Dulkadiroğlu Göksun	4625 4612	Pazarcık	0.46	0.49	0.37	1.835	1.268	0.835	346	ZD
			Nurdağı	0.09	0.11	0.08	0.324	0.357	0.344		
			Elbistan	0.07	0.05	0.04	0.167	0.289	0.110		
			Pazarcık	0.14	0.12	0.06	0.569	0.468	0.223		

Figure 7 Response spectrum and elastic design spectrum acquired from stations 4612, 4614, 4616, and 4625 located in Kahramanmaraş during the earthquakes

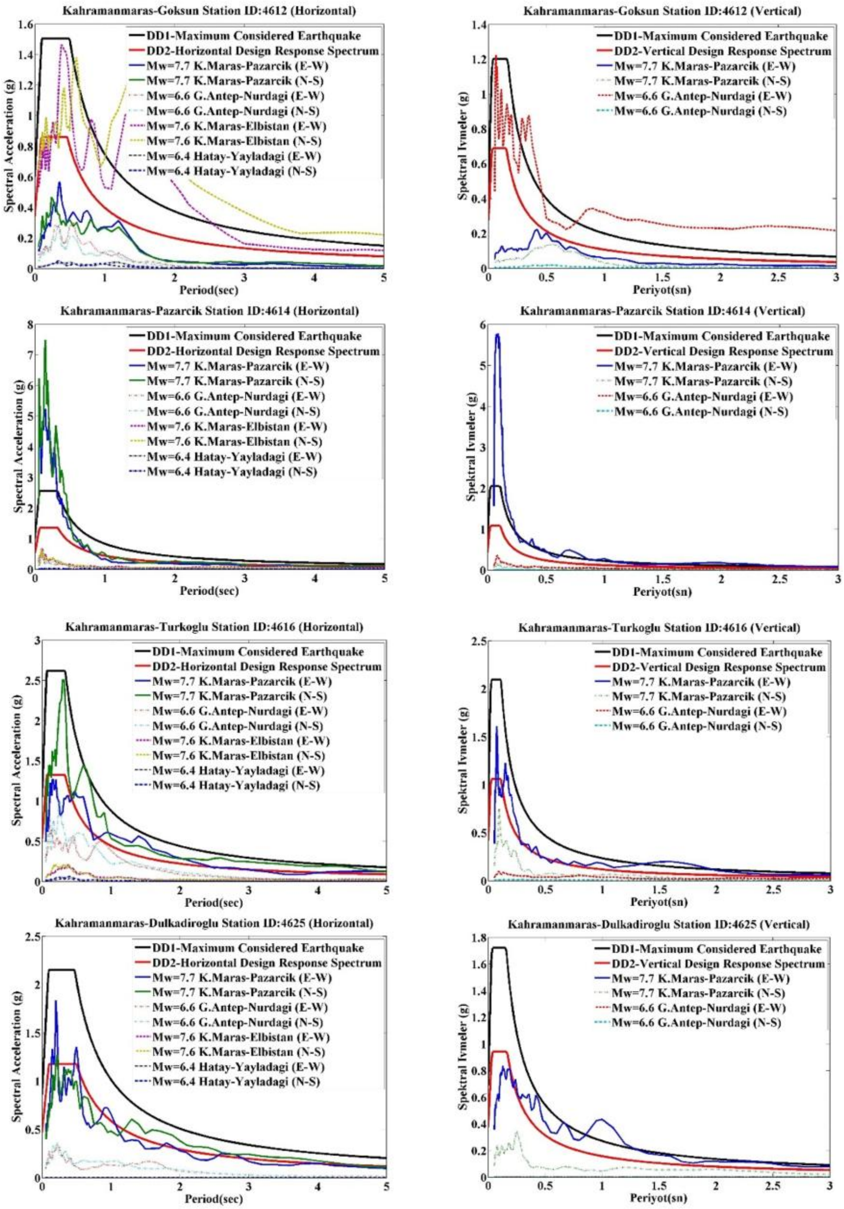

Kilis

The peak ground acceleration value in Kilis during these earthquakes was read as 0.20g in the east-west direction by the accelerometer placed in the Central district numbered 7912 during the Nurdağı earthquake. The largest ground accelerations (PGA) and the largest response spectrum accelerations of the Kilis Central district are given in Table 9, and the comparison of the response spectrum with the elastic design spectrum is given in Figure 8. As shown in Figure 8, the spectral accelerations caused by the earthquake in Kilis province are generally below the elastic design spectrum accelerations defined in TBEC-2018.

Table 9 Peak ground acceleration and response spectrum values for Kilis

City	District	Sta. No	Earthquake	max PGA (g)			max S_{ae} (g)			$(V_s)_{30}$ m/s	Soil class
				EW	NS	UD	EW	NS	UD		
Kilis	Merkez	7901	Pazarcık	0.05	0.02	0.05	0.081	0.106	0.121	463	ZC
			Nurdağı	**0.20**	**0.12**	**0.07**	**0.540**	**0.677**	**0.341**		
			Elbistan	0.05	0.05	0.02	0.155	0.179	0.073		
			Yayladağı	-	-	-	-	-	-		

Figure 8 Response spectrum and elastic design spectrum acquired from station 7901 located in Kilis during the earthquakes

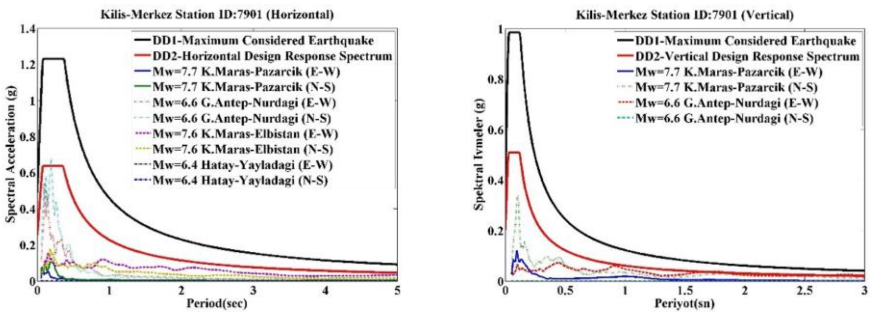

Şanlıurfa

The peak ground acceleration value in Şanlıurfa, which was affected by these earthquakes, was read as 0.24g in the northwest direction by the accelerometer placed in the Central district numbered 6304 during the Pazarcık earthquake. The largest ground accelerations (PGA) and the largest response spectrum accelerations of Şanlıurfa Central district are given in Table 10, and the comparison of the response spectrum with the elastic design spectrum is given in Figure 9. According to Figure 9, the spectral accelerations taken from station 6304 in Şanlıurfa province are generally above the elastic design spectrum accelerations defined in TBEC-2018.

Table 10 Peak ground acceleration and response spectrum values for Şanlıurfa

City	District	Sta. No	Earthquake	max PGA (g)			max S_{ae} (g)			$(V_s)_{30}$ m/s	Soil class
				EW	NS	UD	EW	NS	UD		
Ş.urfa	Merkez	6304	Pazarcık	0.22	0.24	0.09	0.811	0.711	0.295	376	ZC
			Nurdağı	0.04	0.05	0.02	0.148	0.141	0.055		
			Elbistan	-	-	-	-	-	-		
			Yayladağı	-	-	-	-	-	-		

Figure 9 Response spectrum and elastic design spectrum acquired from station 6304 located in Şanlıurfa during the earthquakes

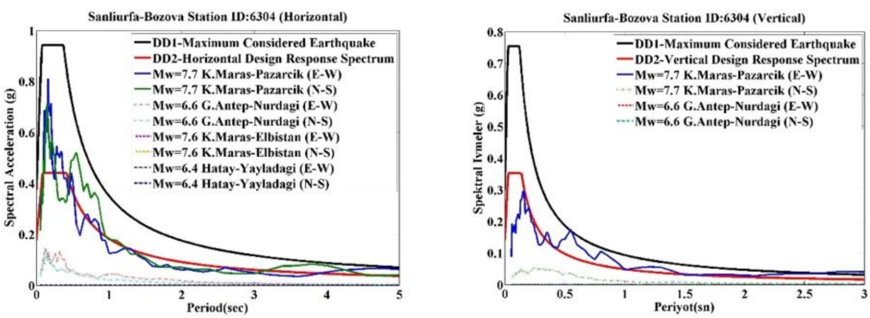

Osmaniye

The peak ground acceleration value in Osmaniye, where there was destruction as a result of these earthquakes, was read as 0.34g in the vertical direction by the accelerometer placed in Bahçe district number 8002 in the Pazarcık earthquake. The largest ground accelerations (PGA) and the largest response spectrum accelerations of Osmaniye Bahçe and Central districts are given in Table 11, and the comparison of the response spectrum with the elastic design spectrum is given in Figure 10. As indicated in Figure 10, the spectrum accelerations of station 8002 in Osmaniye, Bahçe exceed the elastic design spectrum accelerations determined according to TBEC-2018 principles in regions where the period is approximately 0.5 - 2.0 seconds.

Table 11 Peak ground acceleration and response spectrum values for Osmaniye

City	District	Sta. No	Earthquake	max PGA (g)			max S_{ae} (g)			$(V_s)_{30}$ m/s	Soil class
				EW	NS	UD	EW	NS	UD		
Osmaniye	Bahçe	8002	Pazarcık	**0.25**	**0.21**	**0.34**	0.601	**0.857**	**1.104**	430	ZC
			Nurdağı	0.13	0.17	0.13	0.613	0.477	0.395		
			Elbistan	0.07	0.05	0.03	0.156	0.255	0.116		
			Yayladağı	-	-	-	-	-	-		
	Merkez	8003	Yayladağı	-	-	-	-	-	-	350	ZD
			Pazarcık	0.14	0.19	0.14	**0.642**	0.423	0.413		
			Nurdağı	0.06	0.07	0.05	0.211	0.172	0.154		
			Elbistan	0.05	0.07	0.03	0.180	0.156	0.121		

Figure 10 Response spectrum and elastic design spectrum acquired from stations 8002 and 8003 located in Osmaniye during the earthquakes

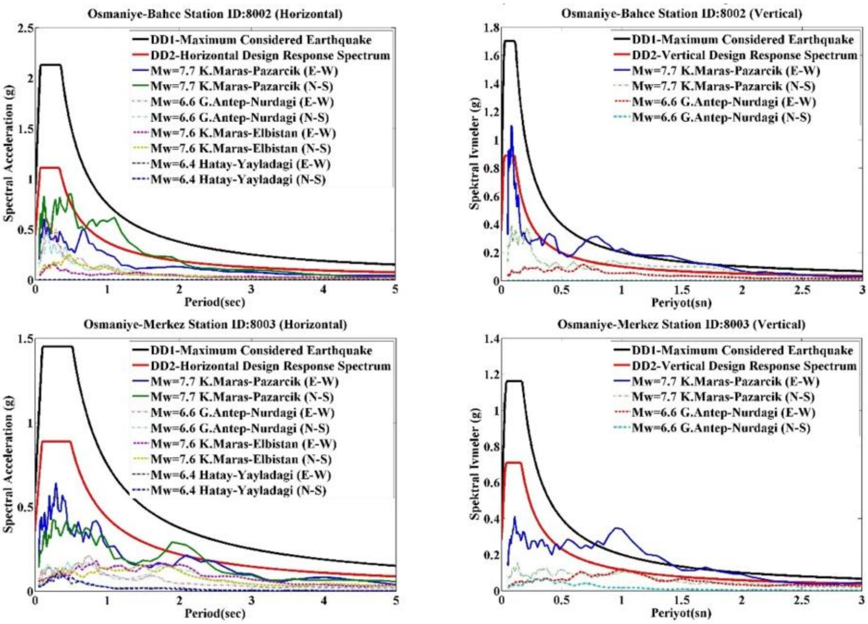

Within the scope of this study, the examined stations were the first 100 stations where the greatest ground acceleration (PGA) values were measured at AFAD stations after the Kahramanmaraş Pazarcık earthquake with M_w 7.7 magnitude, Gaziantep Nurdağı earthquake with M_w 6.6 magnitude, Kahramanmaraş Elbistan earthquake with M_w 7.6 magnitude and Hatay Yayladağı earthquake with magnitude M_w 6.4. Elastic design spectrum were prepared according to TBEC-2018 principles by using response spectrum with a 5% damping rate using ground accelerations and ground classes corresponding to $(V_s)_{30}$ values at each relevant station. When the obtained response spectrum are compared with the elastic design spectrum, it is shown that there is no exceedance in Kilis, there is partial exceedance in Adana, Diyarbakır, and Osmaniye, but there are serious exceedances in Adıyaman, Gaziantep, Hatay, Malatya, and Kahramanmaraş. The peak level of destruction occurred in Hatay and Kahramanmaraş provinces. The spectrum accelerations obtained for these provinces are approximately 5 times the spectral acceleration value defined in the regulation. Accordingly, the necessity of urgently updating the Türkiye Earthquake Hazard Map has emerged.

Causes of Damages in RC Residential Buildings

In the seismic zone, 87% of the buildings are RC structures which generally have frame systems with columns, beams, and floors. Earthquake damage has always been an interesting topic for researchers to guide their future studies and learn from the past. RC structure damages can generally be examined under two main headings: mistakes in the design phase and application phase. In this section, the RC structure damages in the provinces affected by the earthquakes centered in Kahramanmaraş are discussed in detail under the relevant headings.

Soft/weak story damages

The ground floors of buildings in city center of Turkey are mostly commercial areas. Removing the infill walls to create a larger area on these floors reduces the rigidity of the load-bearing systems. This situation causes large displacements on the floor due to seismic forces. Figure 11 shows buildings damaged due to soft story in Kahramanmaraş, Gaziantep, and Hatay provinces. Collapse due to the presence of soft story is one of the damage types frequently observed in many earthquakes that have occurred in recent years [43]. Soft story irregularity does not always mean poor performance. However, if the ductility demands are not met in the design and the inter-story drifts are not limited, a local collapse mechanism or a story failure mechanism may occur.

Figure 11 Observations of damage due to soft/weak story irregularity

(a)Kahramanmaraş *(b)Gaziantep-Nurdağı* *(c)Hatay*

Infill wall damages

Infill wall damage is the most observed type of damage in RC buildings in Turkey. This damage consists of interface cracking, diagonal cracking, and crushing at the frame boundary interfaces. Figure 12 shows infill wall damage examples observed in Adana, Osmaniye, Hatay, and Gaziantep provinces. Although infill walls are not considered as structural elements in practice, their dynamic behavior is crucial because they interact with the RC system. Considering the damage suffered by infill walls after the earthquake, it is obvious that they contribute to energy absorption and horizontal load resistance.

Figure 12 Observations of infill wall damages

(a)Adana *(b)Osmaniye* *(c)Gaziantep-Nurdağı* *(c)Hatay*

Damages caused by heavy overhangs

The upper floor plan areas of some buildings differ significantly due to the presence of overhangs. Overhangs made using cantilever beams that carry heavy wall loads are elements that pose a danger to structures in every earthquake. There is no vertical load-bearing element to prevent the lateral translation of the walls on the cantilever beams. For this reason, severe overhang damage occurs. Figure 13 shows the damages caused by heavy overhangs in Osmaniye and Kahramanmaraş provinces. In addition, during an earthquake, cantilever beams suffer serious damage because they lack sufficient rigidity. In areas with overhangs, beams are frequently not built due to architectural concerns, resulting in a lack of beam-column joints. This situation negatively affects the load transfer mechanism. Damages may occur in overhangs due to vertical earthquake accelerations.

Figure 13 Heavy overhang damages

(a) Osmaniye

(b) Kahramanmaraş

Column and shear wall damages

The columns and shear walls that make up the vertical load-bearing system are crucial elements in terms of maintaining the stability of the structure during the earthquakes. To absorb the shear force that may occur during the earthquake, there must be used sufficient amount, diameter and spacing of stirrups, and concrete with sufficient strength. The wall damages usually occur as X-shaped shear cracks. These damages increase proportionally with the number of floors and height of the building. If the shear wall is weak and the end area is strong, shear cracks occur in the body area. If the column end members are weak and there is no stirrup tightening, large pressure forces occur in the columns due to buckling of the shear wall. Therefore, compressive forces may cause crushing. In addition, insufficient tightening results in buckling of the longitudinal reinforcement in both elements. Columns and shear walls damages observed during field studies are presented in Figure 14.

Figure 14 Columns and shear walls damages

(a)Hatay *(b)Osmaniye* *(c)Gaziantep-Nurdağı* *(c)Kahramanmaraş*

Damages caused by structural system irregularities

Structural system selection of RC structures is crucial in terms of earthquake behavior. The presence of a sufficient number and size of vertical load-bearing elements in the system increases the horizontal resistance capacity. In addition, the symmetrical, regular, and continuous bearing elements are among the most important parameters of earthquake-resistant building design. It is important for the structure load transfer system that the columns and shear walls are approximately equal in both directions in the plan and that the columns are surrounded by beams in both directions. Additional shear walls must be placed to prevent the shear walls placed around elevators and stairs from moving the center of rigidity away from the center of mass. Figure 15 shows the structural system irregularities of RC structures built in seismic zones. The fact that the geometric plans preferred in these buildings are not simple, regular, and symmetrical and the lack of continuous axes are the problems that are noticeable at first glance.

Figure 15 Examples of buildings with structural system irregularities

(a)Adana *(b)Kahramanmaraş* *(c)Osmaniye*

Strong beam-weak column damages

Beams are required to undergo deformation before columns to ensure that the structures remain stable under horizontal loads. In order to ensure the strong column weak beam principle, TBEC-2018 requires the column capacity to be at least 20% more than the total capacity of the beams connected to that column, which is one of the main principles of ductile design. Due to some architectural requirements and different reasons, the beams may be larger than the column and are built together with the floor, resulting in high bearing capacity. Column damages before the beams directly affect the stability of the entire structure. For this reason, beams must be designed to be more ductile than columns. In this case, under dynamic influence, the columns undergo plastic hinges before the beams, resulting in partial or total collapse. Damages caused by strong beams and weak columns observed in Hatay and Kahramanmaraş provinces are given in Figure 16.

Figure 16 Strong beam-weak column damages

(a) Osmaniye *(b) Kahramanmaraş*

Short-column damages

In buildings, the short column effect occurs during an earthquake due to ribbon windows, discontinuities in floor beams, and non-load-bearing rigid elements shortening the effective length of columns. The decrease in the net height of the column and the increase in lateral stiffness cause it to be exposed to more than the expected shear force. This may cause serious shear damage to the columns. Short-column damages observed in the seismic zone are presented in Figure 17.

Figure 17 Short column damages

(a)Kahramanmaraş *(b)Gaziantep-Nurdağı* *(c)Osmaniye* *(d)Kahramanmaraş*

Improper expansion joint damages

In our country, there are many adjacent buildings with insufficient expansion joint distances due to architectural and economic reasons. The floor height, building weight, and stiffness of adjacent regular structures differ the dynamic characteristics of the structures. This situation distances the dynamic periods of the structures from each other. These structures with different dynamic behaviors collide with each other due to insufficient joint distance during an earthquake is called the hammering effect. Hammering damages were encountered in many places during field studies, the damages are presented in Figure 18.

Figure 18 Damages due to insufficient joint distances

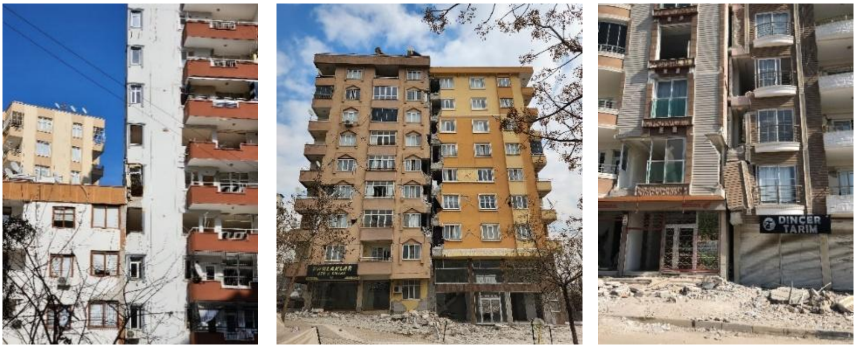

(a)Adana *(b)Kahramanmaraş* *(c)Hatay*

Corner column damges

The damage type suffered by unconfined columns that cannot be connected to the frame system of the building due to heavy overhangs during the earthquake is called corner column damage. This damage type usually occurs as a chain collapse of the section around the corner column from the upper floors to the lower floors. Due to the high slab bending capacity, this type of damage can sometimes spread to other parts of the building. Figure 19 shows corner column damage types observed in Adana, Hatay, and Gaziantep provinces.

Figure 19 Corner column damages

(a)Adana (b)Gaziantep-Nurdağı (c)Hatay

Inadequate stirrup properties and over-lapping length damages

All earthquake regulations from the 1975 earthquake regulation to the present day have focused on the arrangement of stirrups. There are various limitations in the regulations on stirrup densification spacing and length, hook angles, and number of arms. In many cities affected by the Kahramanmaraş earthquakes, the primary reason for structural damages is the improper stirrup properties. It has been determined that the longitudinal reinforcements of many new buildings built in 2018 and later were buckled due to insufficient stirrup spacing and hook angles in the connections from the basement shear wall to the ground floor column. In addition, overlapping and interlocking lengths are crucial to ensure continuity between floors.

During the earthquake, it was observed that sufficient adherence could not be achieved due to short and insufficient stirrup usage at overlaps, and the reinforcement was stripped, resulting in structural damage and collapse (Figure 20). While stirrup hook angles were specified as 135o in all regulations from 1975 onwards, the hook angles in many structures were 90o (Figure 20c). Additionally, shear cracks were observed in many structural elements due to the presence of insufficient stirrups in the densification areas. These deficiencies prevented the ductile behavior and caused the brittle damage presented below (Figure 21).

Figure 20 Improper over-lapping and stirrup hook angle

(a)Adana *(b)Osmaniye* *(c)Kahramanmaraş*

Figure 21 Inadequate stirrup spacing

(a)Osmaniye *(b)Kahramanmaraş* *(c)Adana*

Column-beam joint damages

During seismic events, the effects of horizontal forces are concentrated in the column-beam joints. In this case, shear stresses and bending moments occurring in the joint areas may reach limit values. Column-beam joint areas must have sufficient strength and ductility to absorb these effects and consume earthquake energy. Serious damages may occur in the joint areas due to the poor concrete and improper stirrup arrangement. During field studies, many column-beam joint damages were observed (Figure 22). Damages occurring in the column-beam joints may cause partial or total collapse of the structures.

Figure 22 Column-beam joint damages

(a)Kahramanmaraş *(b)Hatay* *(c)Osmaniye*

Beam damages

Flexural and shear cracks are frequently encountered in beams. The basis of these damages is due to inadequate stirrup, longitudinal reinforcement arrangement and inadequate overlapping length. In addition, the cracks occur in the support region due to the stud beams, which are frequently encountered especially in residential-type buildings. Figure 23 shows the beam damages occurring in Osmaniye, Hatay, Gaziantep, and Kahramanmaraş provinces.

Figure 23 Beam damages

(a)Osmaniye *(b)Hatay* *(c)Gaziantep-Nurdağı* *(d)Kahramanmaraş*

Application phase mistakes

One of the most important factors in the earthquake behavior of RC structures is concrete quality. The concrete strength accepted in the project may deviate due to reasons such as the use of dirty materials in concrete, inappropriate grain size, and distribution, adding extra water during the concrete pouring stage, and careless workmanship. During field studies, traces of carbonation were frequently found in porous and hand-crumble concretes with high permeability in Adana, Kahramanmaraş, and Gaziantep provinces. In addition, in the examinations carried out, especially in areas close to the sea and river shores, concretes using large flat-round shaped aggregate particles were found (Figure 24).

Figure 24 Damage due to insufficient concrete strength and improper aggregate usage

(a)Osmaniye *(b)Kahramanmaraş* *(c)Gaziantep-Nurdağı* *(d)Adana*

The most important element required for RC to exhibit a composite structure behavior is to ensure full adherence between concrete and reinforcement. In this case, there will be a constant force transfer between the concrete and the reinforcement, working together. The corrosion is frequently seen in coastal cities, on building exteriors and basements, or in the reinforcement of RC elements where salty sea sand is used. corrosion was generally found in the reinforcement of the load-bearing elements in the basement and on the exterior. Especially in the Adana-Çukurova region, corrosion has been frequently encountered due to the high groundwater level and humidity level of the air in the region. The corroded reinforcements reached a brittleness that could be crumbled by hand, their diameters decreased, and they lost ductile behavior property. Additionally, the stirrups that lost their function during the earthquake opened/ruptured and caused buckling in the longitudinal reinforcement of the columns (Figure 25). The investigations reveal that the thickness of the cover should be evaluated by taking into account the environmental conditions in the region of the building. In addition, the importance of drainage and bundling processes was also revealed in this earthquake.

Figure 25 Corrosion damages

(a)Osmaniye *(b)Kahramanmaraş* *(c)Gaziantep-Nurdağı* *(d)Adana*

RC structures are generally damaged due to materials, workmanship, soil type, incorrect design, lack of inspection, and lack of necessary maintenance and repair. For this reason, the structures must be flawlessly designed, constructed, and implemented. When the structures that were damaged and collapsed during the earthquakes were examined, workmanship mistakes were found at all stages, especially in concrete and reinforcement workmanships. In Figure 26a and b, it is observed that the installation pipes were passed through the beam, causing severe damage to the beam. Figure 26c shows the cold joints and corroded reinforcements that occurred because of careless stair landing and stair arm connection observed in Kahramanmaraş province. In addition, damage due to the lack of reinforcement in the lower areas of the stairs where connected to the landing is frequently observed. The placement of longitudinal reinforcements, their quantities, and surrounding them with stirrups are crucial. Figure 26d shows the damage caused by longitudinal reinforcement that is not surrounded by stirrups due to workmanship mistakes. Due to the use of stirrups with insufficient spacing, incorrect hook angle and length, non-ductile behavior, and shear fractures occur in the carrier system elements. Figure 27 shows damage caused by incorrect hook angle and excessive stirrup spacing.

Figure 26 Workmanship mistakes

(a)Osmaniye-Düziçi *(b)Gaziantep-Nurdağı* *(c)Kahramanmaraş* *(d)Adana*

Figure 27 Incorrect stirrup hook angle and buckling of longitudinal reinforcement

(a)Osmaniye *(b)Hatay* *(c)Kahramanmaraş* *(d)Adana*

Load bearing system discontinuity

For seismic loads to be safely carried, continuous frame systems should be constructed, and load-bearing elements must be fully connected. Discontinuities in the load-bearing system may occur in structures due to architectural concerns or engineering negligence. Past earthquakes have clearly demonstrated the destructive effects of such discontinuities. Field investigations conducted after the Kahramanmaraş earthquakes and the obtained formwork plans indicate that such discontinuities are widespread and have significantly contributed to the collapse of structures. (Figure 28)

Figure 28 Load-Bearing System Discontinuities Observed in the Kahramanmaraş Earthquakes

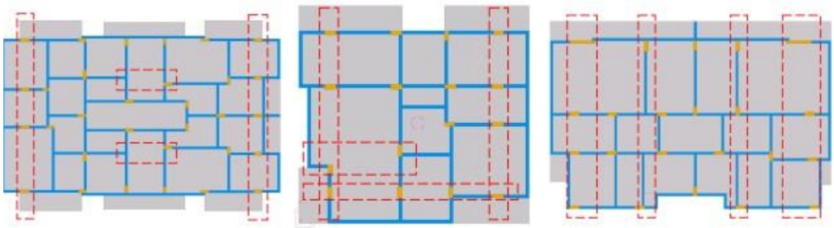

Case Study of the Building Damaged in the Pazarcık Earthquake

The building in examination, which was designed in compliance with the 1975 Turkish Earthquake Code and constructed in 1990, collapsed during the earthquake that occurred on February 6, 2023. The structure consists of a ground story and four normal story, with a total height of 15.3 meters. The height of the ground story is 3.7 meters, while the other stories have a height of 2.9 meters each. The ground story is designated for commercial use. The formwork plan and 3D ETABS model of the structure are presented in Figures 1. The structure was modeled in the ETABS program based on the existing archival project. The concrete class of the structure was determined through core samples taken from the building. In Turkey, older structures with ground stories designated for commercial use typically exhibit infill wall ratios between consecutive stories that do not comply with the thresholds defined in the building codes. This situation increases the likelihood of weak/soft story irregularity occurring in the examined structure. Despite the structural design indicating a concrete class of C14, tests conducted on core samples demonstrated that the existing concrete strength is merely 8 MPa. The rebar class was determined as S220. Upon examining the formwork plan presented in Figure 29, it is evident that frame discontinuities are present. In addition, significant variations in column dimensions were identified; while the columns on the ground story have a cross-section of 30/80 cm, they were observed to reduce to 25/50 cm on the upper stories. The structure's period in the x-direction is 0.972 seconds, with a modal participation ratio of 78.5%, and in the y-direction, it is 1.374 seconds, with a participation ratio of 81.7%.

Figure 29 Structure Model: Formwork Plan of the Investigated Structure - 3D ETABS Model of the Investigated Building

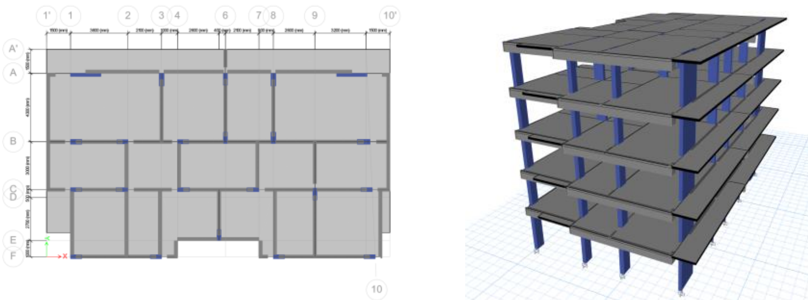

(a)Formwork Plan *(b)3D ETABS Model*

Determination of nonlinear behavior of structural elements (Plastic Hinge Hypothesis)

In the nonlinear analysis of structures, lumped and distributed plastic hinge models are utilized to model the nonlinear behavior of structural elements (Figure 30). These models are based on the assumption that nonlinear deformations are typically concentrated at the ends of the elements or within a specific region. The plastic hinge length (Lp) is assumed to be equal to half of the cross-sectional dimension in the direction of interest (h) ($Lp \approx 0.5h$) (TBEC 2018). The lumped plastic hinge model is preferred for cases where damage is concentrated at the ends of the elements rather than distributed along their length, while the distributed plastic hinge model is used for situations where damage is spread throughout the element or over a specific portion of its length (Deierlein et al. 2010). In the nonlinear analysis of frame structures, lumped plasticity has long been an accepted method; however, with advancements in computer technology, the distributed plasticity approach has also gained significance and its application has expanded.

Figure 30 Nonlinear Behavior Models for Structural Analysis

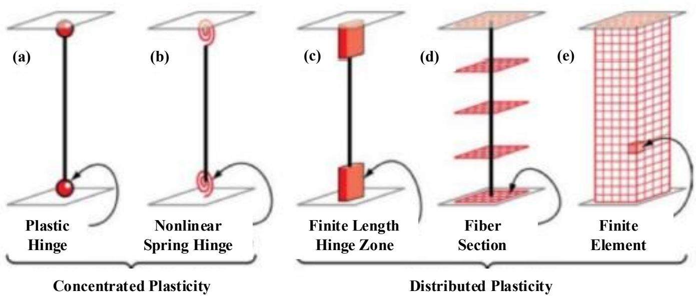

Figure 31 illustrates the three fundamental limits in plastic hinges: Immediate Occupancy (IO), Life Safety (LS), and Collapse Prevention (CP). The Immediate Occupancy limit defines the point at which the element transitions from elastic behavior to plastic deformation. The Life Safety limit represents the boundary within which the element can safely sustain its strength while exhibiting plastic behavior. The Collapse Prevention limit marks the final stage where the element completely loses its functionality and is at risk of failure.

Figure 31 Accepted Damage Regions for Plastic Hinges

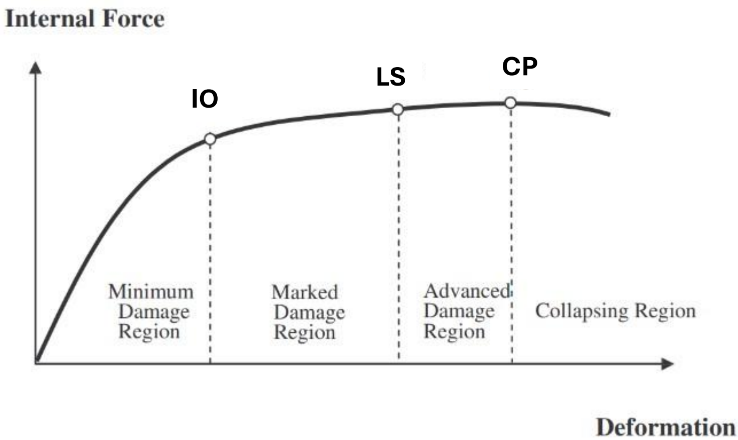

Nonlinear time history analysis for the investigated building

The acceleration records of the earthquake that occurred on February 6, 2023, were obtained from Station 3126, the closest station to the structure (Figure 32). The acceleration-time, velocity-time, and displacement-time graphs, along with the response spectrum plots, are shown in Figures 33-8. The East-West, North-South, and vertical components obtained from Station 3126 were directly applied to the structure in the ETABS program. All three components were simultaneously imposed on the structure at the same time. By rotating the horizontal components by 90º, the analysis was conducted again, and the worst-case scenario was determined and reported. The results obtained within the scope of the study were evaluated in terms of story displacements, story drift, story forces, story accelerations, torsional irregularity, and performance-based design parameters. In the structural analysis, the lumped plasticity hinge model available in the ETABS software was adopted as the plastic hinge model. Within the scope of this model, the nonlinear behavior of structural elements was modeled in accordance with the acceptance criteria specified in the ASCE 41-13 standard. These criteria are defined based on the limit values and performance levels provided in Table 10-7 for beams and Table 10-8 for columns in the ASCE 41-13.

Figure 32 The Distance Between the Structure and the Accelerograph Station

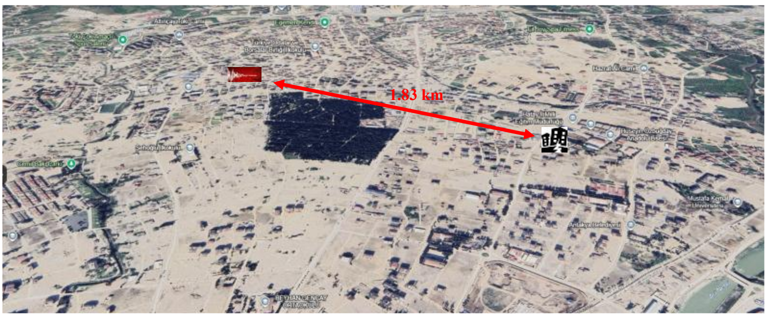

Figure 33 East-West Component of the Record Obtained from Station 3126

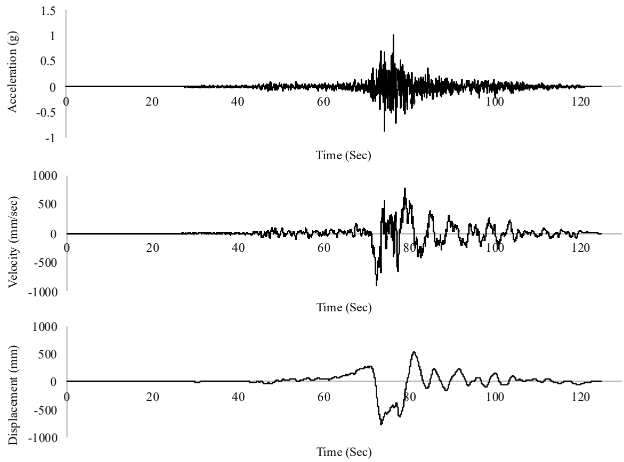

Figure 34 North-South Component of the Record Obtained from Station 3126

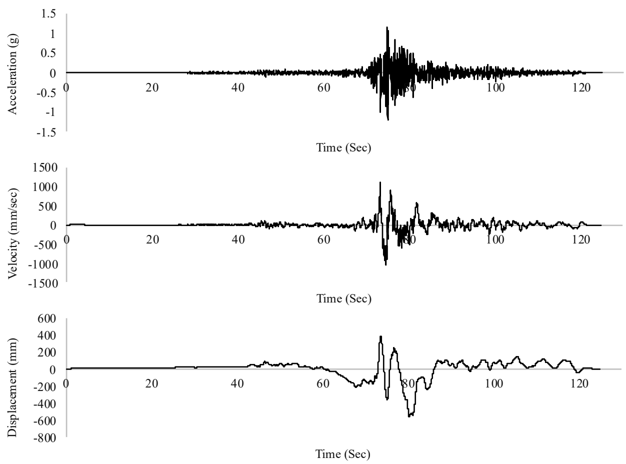

Figure 35 Vertical Component of the Record Obtained from Station 3126

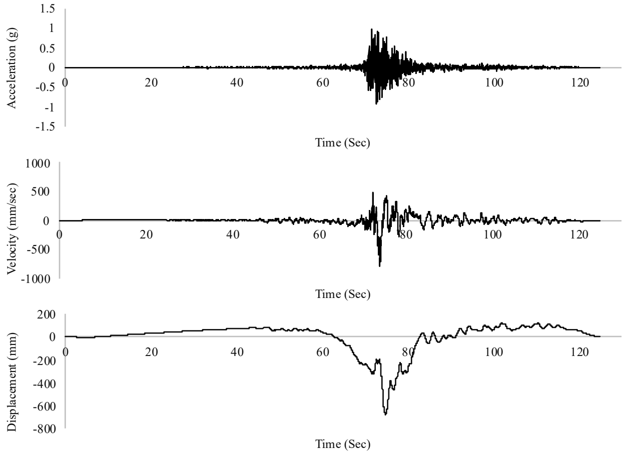

Figure 36 Response Spectra of the Acceleration Record Components

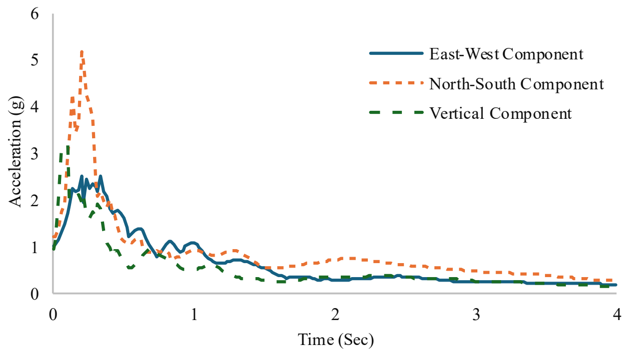

Results of the time history analysis

When examining the story displacements, it was determined that the displacement values at the roof level of the structure exceeded 400 mm (Figure 37). In terms of story drifts, it was observed that the drift ratio reached nearly twice the critical threshold of 2% (Figure 38). The acceleration experienced at the roof level was found to be above 4g (Figure 40). Additionally, torsional irregularity was identified in the structure, with the limit value of 1.2

specified in TBEC 2018 being exceeded by 21.5% (Table 12). When the performance analysis results are examined, it is concluded that the presence of two brittle column elements on each story increases the risk of collapse of the structure. Additionally, significant damage was observed in the beam elements due to inadequate column-beam connections (Table 13-Figure 41).

Figure 37 Story Displacements

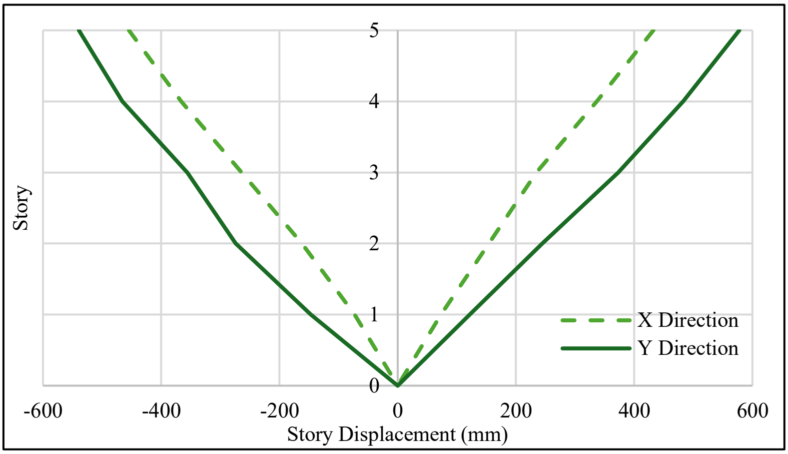

Figure 38 Story Drifts

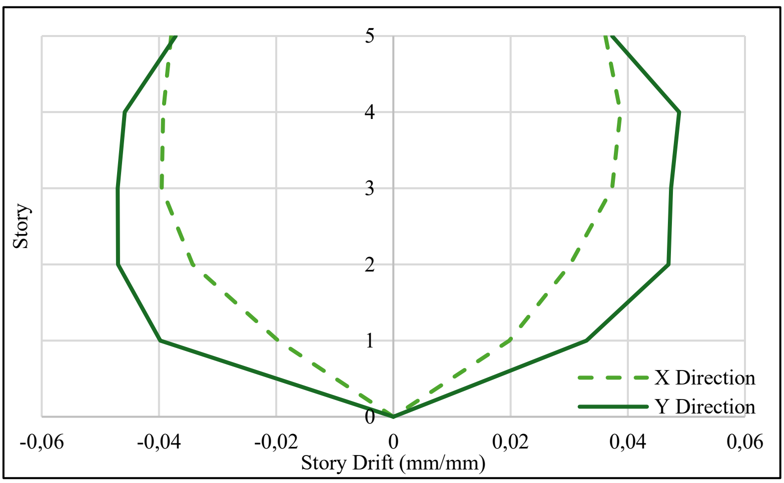

Figure 39 Story Forces (Shear Forces)

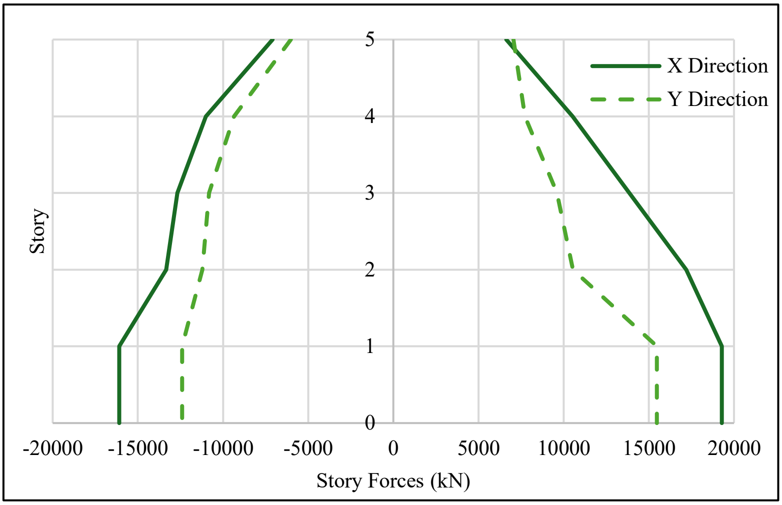

Figure 40 Story Accelerations

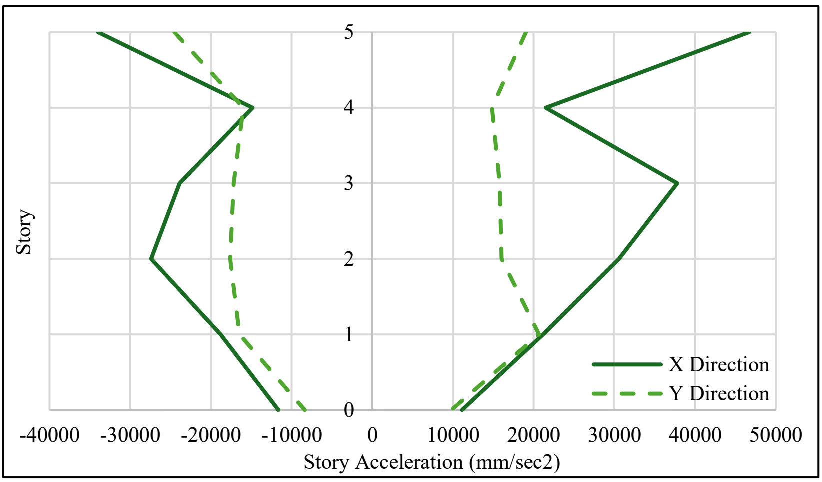

Table 12 Torsional Irregularity Is Checked According to TBEC 2018

	X Direction				Y Direction			
Story	**Max Drift**	**Max Avg Drift**	**Ratio**	**Check**	**Max Drift**	**Max Avg Drift**	**Ratio**	**Check**
5	104.91	71.901	1.46	✕	108.25	94.99	1.14	✓
4	112.36	83.633	1.34	✕	141.42	129.79	1.09	✓
3	108.28	91.621	1.18	✓	137.51	135.24	1.017	✓
2	87.58	79.981	1.09	✓	136.17	127.7	1.07	✓
1	73.30	64.045	1.14	✓	121.95	107.59	1.13	✓

Table 13 Performance Based Design Results

	Column				Beam			
Story	**<IO**	**IO to LS**	**LS to CP**	**CP<**	**<IO**	**IO to LS**	**LS to CP**	**CP<**
5	19	1	0	2	0	48	0	0
4	17	3	0	2	0	48	0	0
3	17	3	0	2	0	48	0	0
2	18	2	0	2	0	48	0	0
1	20	0	0	2	0	48	0	0

Figure 41 Performance Levels of Structural Elements

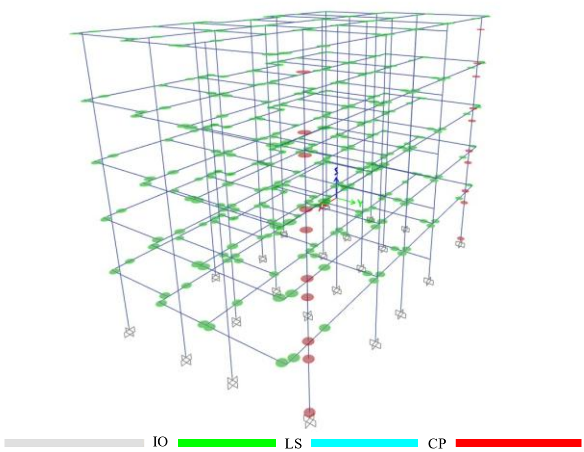

Discussion and Evaluation

Population percentages of the provinces located in the seismic zone are presented in Figure 42. The provinces located in the seismic zone cover 16.4% of the country's population (Figure 43). Among these provinces, the province with the most population is Adana, and the least populated is Kilis.

Figure 42 Population percentages of the provinces in the seismic zone [46]

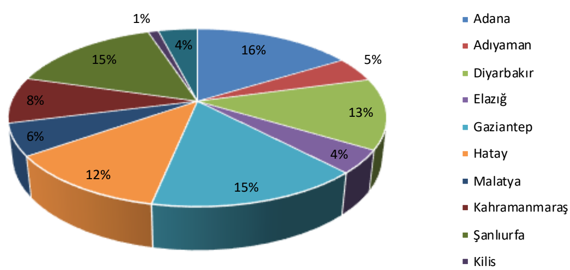

Figure 43 Seismic zone population compared to the rest of the country [46]

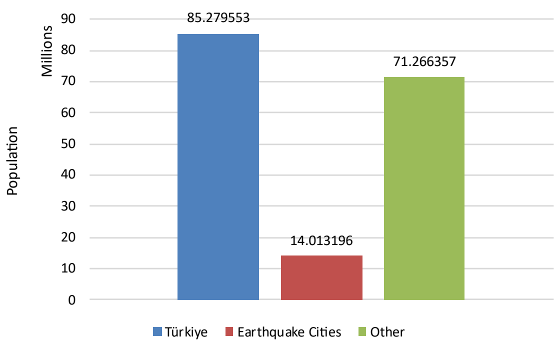

The ratios of the buildings in the provinces affected by the earthquake according to intended use are given in Figure 44. Accordingly, 89.1% of the 2.618.697 registered buildings are residential, 6.2% are workplaces, 2.8% are public and 1.9% are other buildings. Province-based percentages of structures affected by the earthquake are given in Figure 45. Accordingly, the province with the most buildings is Adana, and the provinces with the least buildings are Osmaniye and Kilis.

Figure 44 Building types in the seismic zone [47]

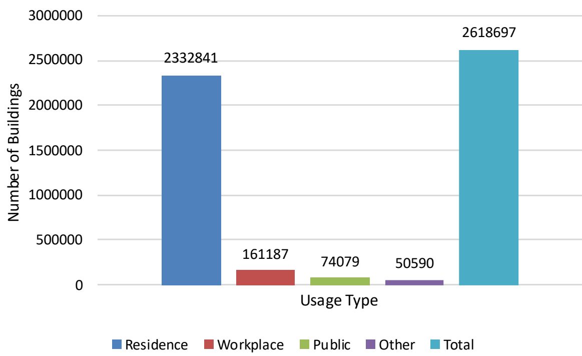

Figure 45 Province based percentages of buildings in the seismic zone [47]

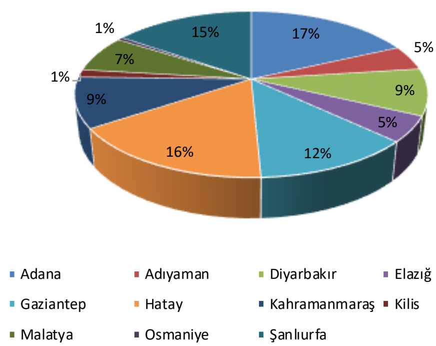

Immediately after the earthquake, damage assessment studies were carried out by the Ministry of Environment, Urbanization, and Climate Change. Figure 46 shows the percentages of the structural conditions obtained in the damage assessment study conducted on March 6, 2023. However, approximately 50% of the structures in the region could not be identified initially. According to the findings, 2%

of the buildings were found to be undamaged, 25% were slightly damaged, 2% were moderately damaged, 11% were heavily damaged, 9% were destroyed, and 1% were to be demolished urgently.

Figure 46 Damage assessment status [48]

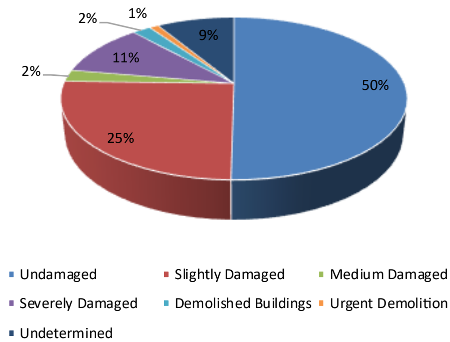

The construction date of building is a substation parameter in the building evaluation because that determines if deformed reinforcement and ready-mixed concrete technology were used. Also, according to construction date, which earthquake regulation was followed and whether the building inspection system was applied are known. The ratios of the buildings in the provinces in the seismic zone according to their construction dates are presented in Figure 47. In all provinces, most of the building stock consists of buildings built in 2001 and later. Considering the total region, the ratio of buildings built in 2001 and later was 51.1%, while before 2001 it was 37.6%. The year of construction of 11.3% of the buildings is unknown. According to all these ratios, considering the previously mentioned parameters that make the year of construction important, approximately half of the buildings in the region are at risk of not being earthquake resistant.

Figure 47 Ratios of construction years [49]

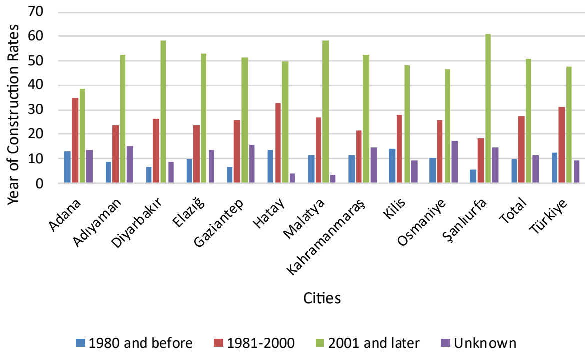

The graph showing the household rates depending on the number of building floors in Türkiye and the provinces in the seismic zone is presented in Figure 48. Approximately 35% of the country's population lives in buildings with 6 or more floors. Among the provinces in the seismic zone, Diyarbakir ranks first in terms of the number of households living in buildings with 6 or more floors, with 49%. Diyarbakır is followed by Gaziantep and Malatya, respectively. Şanlıurfa is the only province where the ratio of single-story buildings exceeds multi-story buildings. Şanlıurfa is the province with the peak density of low-rise construction in the seismic zone.

Figure 48 Household rate according to story number [49]

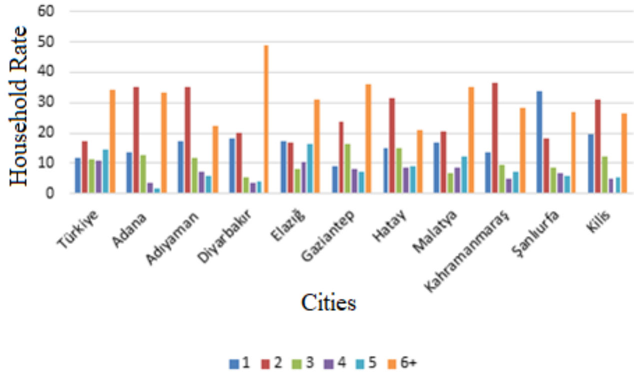

The building stock of the region consists of an 87% RC structural system. The RC system is followed by masonry, prefabricated, other, and steel (Figure 49).

Figure 49 Structural systems in seismic zone [47]

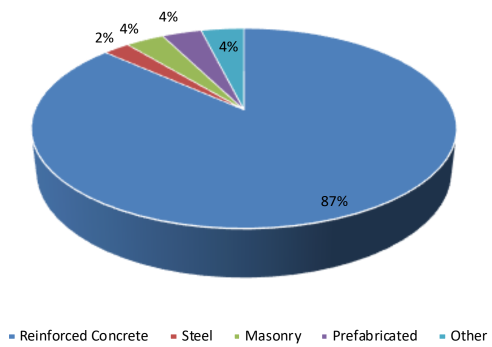

According to damage assessment studies, province-based detection situations are given in Figure 50 in quantity and Figure 51 in proportion. According to the graphs, it can be seen that the greatest destruction and heavily damaged structures are in the provinces of Hatay, Kahramanmaraş, Malatya, and Adıyaman.

Figure 50 Damage assessment status of buildings in the seismic zone [48]

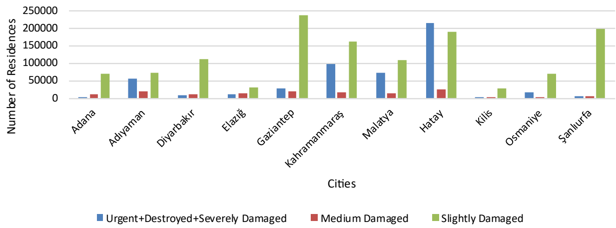

Figure 51 Damage situation of provinces affected earthquake [48]

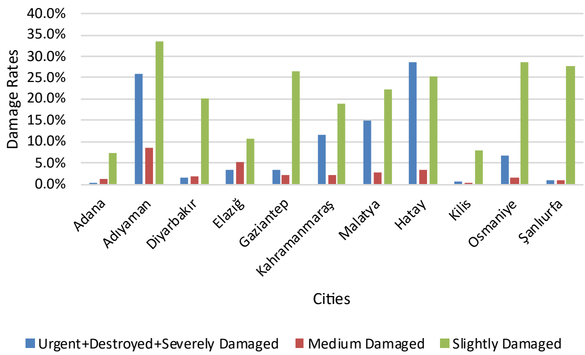

According to the data of the Ministry of National Education, there are a total of 11.699 educational institutions in the earthquake region. 21.4% of the country's student population study and 19.1% of the country's teachers work in these institutions. According to the data of the Council of Higher Education, there are a total of 15 universities in the region. A total of 340.222 students, 17.002 academic staff, and 26.668 administrative staff work in these universities. Within the scope of damage assessment studies for universities, the total number of collapsed buildings in the region is 9, the number of heavily damaged buildings is 111, the number of moderately damaged buildings is 51, and the number of slightly damaged buildings is 358. A total of 281.007 m^2 constitutes the unusable area and 2.122.834 m^2 constitutes the area that needs to be strengthened.

Conclusion

As a result of detailed investigations carried out in the field after the 2023 Kahramanmaraş earthquakes, it was seen that the damages and destructions were caused by mistakes made in the design and application stages and the damage types were similar to the results obtained in previous earthquakes [44]. Structural defects that cause destruction and damage in RC residential buildings can be listed as follows.

- The construction of commercial premises on the ground floor of buildings with high floor heights and without infill walls increases the risk of soft/weak story. The presence of soft/weak story, which is a common type of damage, causes destruction and severe damage in buildings due to inadequate design and deficiencies. It is known that the reduced lateral stiffness of the ground floor, which causes a weak story mechanism, increases the nonlinear shear demands [45]. It has been observed that ground floor collapses occur in many buildings, especially in Hatay and Kahramanmaraş, due to the formation of soft story, that is, weak columns, on the ground floors.
- In all our regulations since the 1975 Earthquake Regulation until today, it is stated that stirrup hooks

must be 135^0 and the length of the stirrup hook is specified. During the field studies, it was observed that stirrup hooks were made 90^0 in almost all buildings completed before 2000 in the provinces examined. In addition, the iron preparations of some structures under construction in the seismic zone were observed, and it was observed that the construction of inappropriate stirrup hook angles was continued. Under the effect of the earthquake, the shell concrete disintegrated, the stirrup hooks were opened, and the longitudinal reinforcements were buckled due to the right-angled hooks and insufficiently spaced stirrups.

- It has been observed that the concrete quality is very low in collapsed and heavily damaged buildings. Aggregates with inappropriate shapes and gradations used in concrete reduce the quality of concrete.
- Buildings constructed adjacently with insufficient joint distances exhibit different dynamic behavior under the influence of earthquakes. Due to insufficient joint space, these structures hit each other during an earthquake and create a hammering effect.
- Proper application in the field is as important as the design and planning of the structures. Damages resulting from various workmanship mistakes were

observed in all of the provinces examined in the earthquake region.

- In the examined structure, lateral displacements exceeding 400 mm at the roof level, story drift ratios reaching nearly twice the critical threshold of 2%, and peak accelerations above 4g at the top story clearly indicate that the structure surpassed the limits of ductile behavior and demonstrated inadequate seismic performance. The brittle failure behavior observed particularly in the corner columns negatively affected the overall stability of the structure and is considered one of the primary causes of its collapse. Due to deficiencies in the beam-column joint regions, damage in both beams and columns extended beyond the minimum damage threshold. Additionally, torsional irregularities—likely resulting from frame discontinuities—exceeded the TBEC 2018 code-defined limit of 1.2 by 21.5%, which adversely affected the behavior of the load-bearing system and triggered localized failures due to the irregular distribution of seismic demands.

In addition, response spectra were prepared for 100 stations where the largest ground accelerations were read, and the results were compared by drawing elastic design spectrum according to TBEC2018 principles. The results obtained showed that earthquake demands were seriously exceeded in Adana, Diyarbakır, and Osmaniye, partly in Adıyaman, Gaziantep, Hatay, Malatya, and Kahramanmaraş. Considering these results, it is recommended to update the Türkiye Earthquake Hazard Map.

Acknowledgements

The authors gratefully acknowledge the support provided by the Scientific and Technological Research Council of Turkiye (TUBITAK), under the program called “1002-C Emergency Support Program for Reconnaissance Study Focusing on Natural Disasters”. Also, the authors gratefully acknowledge the Disaster and Emergency Management Authority (AFAD) of Turkey for providing the strong ground motion records of the stations through their official website.

References

[1] T.R. Presidential Strategy and Budget Directorate, https://www.sbb.gov.tr/ (accessed May 27, 2024).

[2] INSARAG-2023, Team Leaders and Working Groups Meeting 2023 – INSARAG, https://www.insarag.org/insarag-team-leaders-and-working-groups-meeting-2023-2/ (accessed May 27, 2024).

[3] G. Dogan, A.S. Ecemis, S.Z. Korkmaz, M.H. Arslan, H.H. Korkmaz, Buildings Damages after Elazığ, Turkey Earthquake on January 24, 2020, Nat. Hazards 109 (2021) 161–200. https://doi.org/10.1007/s11069-021-04831-5.

[4] M.H. Arslan, H.H. Korkmaz, What is to be learned from damage and failure of reinforced concrete structures during recent earthquakes in Turkey?, Eng. Fail. Anal. 14 (2007) 1–22. https://www.sciencedirect.com/science/article/pii/S135063070600029X (accessed May 27, 2024).

[5] A. Doğangün, Performance of reinforced concrete buildings during the May 1, 2003 Bingöl Earthquake in Turkey, Eng. Struct. 26 (2004) 841–856. https://doi.org/10.1016/j.engstruct.2004.02.005.

[6] E. Işık, F. Avcil, A. Büyüksaraç, R. İzol, M. Hakan Arslan, C. Aksoylu, E. Harirchian, O. Eyisüren, E. Arkan, M. Şakir Güngür, M. Günay, H. Ulutaş, Structural damages in masonry buildings in Adıyaman during the Kahramanmaraş (Turkiye) earthquakes (Mw 7.7 and Mw 7.6) on 06 February 2023, Eng. Fail.

Anal. 151 (2023) 107405. https://doi.org/10.1016/j.engfailanal.2023.107405.

[7] A. Demir, E. Celebi, H. Ozturk, Z. Ozcan, A. Ozocak, E. Bol, S. Sert, F.Z. Sahin, E. Arslan, Z. Dere Yaman, M. Utkucu, N. Mert, Destructive impact of successive high magnitude earthquakes occurred in Türkiye's Kahramanmaraş on February 6, 2023, Bull. Earthq. Eng. (2024). https://doi.org/10.1007/s10518-024-01865-5.

[8] M.L. Ivanov, W.-K. Chow, Structural damage observed in reinforced concrete buildings in Adiyaman during the 2023 Turkiye Kahramanmaras Earthquakes, Structures 58 (2023) 105578. https://doi.org/10.1016/j.istruc.2023.105578.

[9] F. Akar, E. Işık, F. Avcil, A. Büyüksaraç, E. Arkan, R. İzol, Geotechnical and Structural Damages Caused by the 2023 Kahramanmaraş Earthquakes in Gölbaşı (Adıyaman), Appl. Sci. 14 (2024) 2165. https://doi.org/10.3390/app14052165.

[10] H. Sezen, A.S. Whittaker, Seismic performance of industrial facilities affected by the 1999 Turkey earthquake, J. Perform. Constr. Facil. 20 (2006) 28–36. https://doi.org/10.1061/(ASCE)0887-3828(2006)20:1(28).

[11] M.H. Arslan, H.H. Korkmaz, F.G. Gulay, Damage and failure pattern of prefabricated structures after major earthquakes in Turkey and shortfalls of the Turkish Earthquake code, Eng. Fail. Anal. 13 (2006) 537–557. https://doi.org/10.1016/j.engfailanal.2005.02.006.

[12] Z. Celep, A. Erken, B. Taskin, A. Ilki, Failures of masonry and concrete buildings during the March 8, 2010 Kovancılar and Palu (Elazığ) Earthquakes in Turkey, Eng. Fail. Anal. 18 (2011) 868–889. https://doi.org/10.1016/j.engfailanal.2010.11.001.

[13] B. Taskin, A. Sezen, U.M. Tugsal, A. Erken, The aftermath of 2011 Van earthquakes: evaluation of strong motion, geotechnical and structural issues, Bull. Earthq. Eng. 11 (2013) 285–312. https://doi.org/10.1007/s10518-012-9356-9.

[14] A. Bayraktar, A.C. Altunişik, M. Pehlivan, Performance and damages of reinforced concrete buildings during the October 23 and November 9, 2011 Van, Turkey, earthquakes, Soil Dyn. Earthq. Eng. 53 (2013) 49–72. https://doi.org/10.1016/j.soildyn.2013.06.004.

[15] A. Bayraktar, A.C. Altunışık, M. Muvafık, Field Investigation of the Performance of Masonry Buildings during the October 23 and November 9, 2011, Van Earthquakes in Turkey, J. Perform. Constr. Facil. 30 (2016) 04014209. https://doi.org/10.1061/(ASCE)CF.1943-5509.0000383.

[16] G. Milani, Lesson learned after the Emilia-Romagna, Italy, 20–29 May 2012 earthquakes: A limit analysis insight on three masonry churches, Eng. Fail. Anal. 34 (2013) 761–778. https://doi.org/10.1016/j.engfailanal.2013.01.001.

[17] H.B. Ozmen, M. Inel, E. Akyol, B.T. Cayci, H. Un, Evaluations on the relation of RC building damages with structural

parameters after May 19, 2011 Simav (Turkey) earthquake, Nat. Hazards 71 (2014) 63–84. https://doi.org/10.1007/s11069-013-0900-y.

[18] E. Damcı, R. Temur, G. Bekdaş, B. Sayin, Damages and causes on the structures during the October 23, 2011 Van earthquake in Turkey, Case Stud. Constr. Mater. 3 (2015) 112–131.

[19] E. Uckan, B. Akbas, J. Shen, R. Wen, K. Turandar, M. Erdik, Seismic performance of elevated steel silos during Van earthquake, October 23, 2011, Nat. Hazards 75 (2015) 265–287. https://doi.org/10.1007/s11069-014-1319-9.

[20] G. Milani, M. Valente, Failure analysis of seven masonry churches severely damaged during the 2012 Emilia-Romagna (Italy) earthquake: Non-linear dynamic analyses vs conventional static approaches, Eng. Fail. Anal. 54 (2015) 13–56. https://doi.org/10.1016/j.engfailanal.2015.03.016.

[21] A. Demir, T.Y. Altıok, Numerical assessment of a slender structure damaged during October 30, 2020, İzmir earthquake in Turkey, Bull. Earthq. Eng. 19 (2021) 5871–5896.

[22] E. Sayın, B. Yön, O. Onat, M. Gör, M.E. Öncü, E. Tuğrul Tunç, D. Bakır, M. Karaton, Y. Calayır, 24 January 2020 Sivrice-Elazığ, Turkey earthquake: geotechnical evaluation and performance of structures, Bull. Earthq. Eng. 19 (2021) 657–684. https://doi.org/10.1007/s10518-020-01018-4.

[23] R. Temür, E. Damcı, S. Öncü-Davas, C. Öser, S. Sarğın, Ç. Şekerci, Structural and geotechnical investigations on

Sivrice earthquake (Mw = 6.8), January 24, 2020, Nat. Hazards 106 (2021) 401–434. https://doi.org/10.1007/s11069-020-04468-w.

[24] M. Günaydin, B. Atmaca, S. Demir, A.C. Altunişik, M. Hüsem, S. Adanur, Ş. Ateş, Z. Angin, Seismic damage assessment of masonry buildings in Elazığ and Malatya following the 2020 Elazığ-Sivrice earthquake, Turkey, Bull. Earthq. Eng. 19 (2021) 2421–2456. https://doi.org/10.1007/s10518-021-01073-5.

[25] H. Bilgin, N. Shkodrani, M. Hysenlliu, H. Baytan Ozmen, E. Isik, E. Harirchian, Damage and performance evaluation of masonry buildings constructed in 1970s during the 2019 Albania earthquakes, Eng. Fail. Anal. 131 (2022) 105824. https://doi.org/10.1016/j.engfailanal.2021.105824.

[26] N. Ademović, M. Toholj, D. Radonić, F. Casarin, S. Komesar, K. Ugarković, Post-Earthquake Assessment and Strengthening of a Cultural-Heritage Residential Masonry Building after the 2020 Zagreb Earthquake, Buildings 12 (2022) 2024. https://doi.org/10.3390/buildings12112024.

[27] N. Caglar, I. Vural, O. Kirtel, A. Saribiyik, Y. Sumer, Structural damages observed in buildings after the January 24, 2020 Elazığ-Sivrice earthquake in Türkiye, Case Stud. Constr. Mater. 18 (2023) e01886. https://doi.org/10.1016/j.cscm.2023.e01886.

[28] Y.-Y. Ko, C.-C. Tsai, J.-H. Hwang, Y.-W. Hwang, L. Ge, M.-C. Chu, Failure of engineering structures and associated geotechnical problems during the 2022 ML 6.8 Chihshang

earthquake, Taiwan, Nat. Hazards 118 (2023) 55–94. https://doi.org/10.1007/s11069-023-05993-0.

[29] İ. Kazaz, Ö. Avşar, A. Dilsiz, Importance of building inspection on the seismic response of a severely damaged RC structure during the February 6, 2023 Kahramanmaraş earthquake sequence, Eng. Fail. Anal. 162 (2024) 108410. https://doi.org/10.1016/j.engfailanal.2024.108410.

[30] E. Işık, F. Avcil, A. Büyüksaraç, R. İzol, M. Hakan Arslan, C. Aksoylu, E. Harirchian, O. Eyisüren, E. Arkan, M. Şakir Güngür, M. Günay, H. Ulutaş, Structural damages in masonry buildings in Adıyaman during the Kahramanmaraş (Turkiye) earthquakes (Mw 7.7 and Mw 7.6) on 06 February 2023, Eng. Fail. Anal. 151 (2023) 107405. https://doi.org/10.1016/j.engfailanal.2023.107405.

[31] M. Ozturk, M.H. Arslan, G. Dogan, A.S. Ecemis, H.D. Arslan, School buildings performance in 7.7 Mw and 7.6 Mw catastrophic earthquakes in southeast of Turkey, J. Build. Eng. 79 (2023) 107810. https://doi.org/10.1016/j.jobe.2023.107810.

[32] E. Işık, F. Avcil, E. Arkan, A. Büyüksaraç, R. İzol, M. Topalan, Structural damage evaluation of mosques and minarets in Adıyaman due to the 06 February 2023 Kahramanmaraş earthquakes, Eng. Fail. Anal. 151 (2023) 107345. https://doi.org/10.1016/j.engfailanal.2023.107345.

[33] B. Zengin, F. Aydin, The Effect of Material Quality on Buildings Moderately and Heavily Damaged by the

Kahramanmaraş Earthquakes, Appl. Sci. 13 (2023) 10668. https://doi.org/10.3390/app131910668.

[34] Ö. Yıldız, C. Kına, Geotechnical and Structural Investigations in Malatya Province after Kahramanmaraş Earthquake on February 6, 2023, Bitlis Eren Üniversitesi Fen Bilim. Derg. 12 (2023) 686–703. https://doi.org/10.17798/bitlisfen.1282555.

[35] F. Avcil, E. Işık, R. İzol, A. Büyüksaraç, E. Arkan, M.H. Arslan, C. Aksoylu, O. Eyisüren, E. Harirchian, Effects of the February 6, 2023, Kahramanmaraş earthquake on structures in Kahramanmaraş city, Nat. Hazards 120 (2024) 2953–2991. https://doi.org/10.1007/s11069-023-06314-1.

[36] O. İnce, Structural damage assessment of reinforced concrete buildings in Adıyaman after Kahramanmaraş (Türkiye) Earthquakes on 6 February 2023, Eng. Fail. Anal. 156 (2024) 107799. https://doi.org/10.1016/j.engfailanal.2023.107799.

[37] S. Kocakaplan Sezgin, G.B. Sakcalı, S. Özen, E. Yıldırım, E. Avcı, B. Bayhan, N. Çağlar, Reconnaissance report on damage caused by the February 6, 2023, Kahramanmaraş Earthquakes in reinforced-concrete structures, J. Build. Eng. 89 (2024) 109200. https://doi.org/10.1016/j.jobe.2024.109200.

[38] İ. Kocaman, Ö. Mercimek, M. Gürbüz, Y. Erbaş, Ö. Anıl, The effect of Kahramanmaraş earthquakes on historical Malatya Yeni Mosque, Eng. Fail. Anal. 161 (2024) 108310. https://doi.org/10.1016/j.engfailanal.2024.108310.

[39] E. Altunsu, O. Güneş, S. Öztürk, S. Sorosh, A. Sarı, S.T. Beeson, Investigating the structural damage in Hatay province after Kahramanmaraş-Türkiye earthquake sequences, Eng. Fail. Anal. 157 (2024) 107857. https://doi.org/10.1016/j.engfailanal.2023.107857.

[40] V. Kahya, A.F. Genç, F. Sunca, B. Roudane, A.C. Altunişik, S. Yilmaz, M. Günaydin, G. Dok, O. Kirtel, A. Demir, B. Aykanat, M.E. Arslan, A. Saribiyik, F. Aydin, B. Aslan, T. Sezdirmez, T. Tatar, M. Emiroğlu, B. Atmaca, S. Adanur, E. Ertürk Atmaca, O. Güleş, E. Demirkaya, H. Öztürk, T. Akgül, Evaluation of earthquake-related damages on masonry structures due to the 6 February 2023 Kahramanmaraş-Türkiye earthquakes: A case study for Hatay Governorship Building, Eng. Fail. Anal. 156 (2024) 107855. https://doi.org/10.1016/j.engfailanal.2023.107855.

[41] O.C. Celik, M.B.C. Ulker, C. Gocer, S. Guntepe, O. Koz, M.M. Eyupgiller, M. Aksu, A. Yaz, Multidisciplinary reconnaissance investigation covering structural, geotechnical, and architectural based damage to mid-rise residential buildings following the February 6th, 2023 Kahramanmaraş, Türkiye earthquake doublets (Mw 7.8, Mw 7.6), Soil Dyn. Earthq. Eng. 182 (2024) 108738. https://doi.org/10.1016/j.soildyn.2024.108738.

[42] Turkish Building Earthquake Code-2018 (TBEC), Ministry of Public Works and Settlement, Ankara.

[43] C. Scawthorn, The Marmara, Turkey Earthquake of August 17, 1999: Reconnaissance Report, in: Marmara Turk. Earthq.

August 17 1999 Reconnaiss. Rep., 2000: pp. 190–190. https://pesquisa.bvsalud.org/portal/resource/pt/des-12613 (accessed June 6, 2024).

[44] A. Demir, A. Özyüksel Çiftçioğlu, B. SINIR, E. Basari, E. Dogan, H. Nohutcu, M. Bozkurt, R.T. Erdem, T. Altıok, İzmir (Seferihisar-Sisam) Depreminin Sismik Karakteristiği ve Meydana Gelen Yapısal Hasarların İncelenmesi, 2020. https://doi.org/10.13140/RG.2.2.14481.66402/1.

[45] N. Kirac, M. Dogan, H. Ozbasaran, Failure of weak-storey during earthquakes, Eng. Fail. Anal. 18 (2011) 572–581. https://www.sciencedirect.com/science/article/pii/S1350630710001731 (accessed June 6, 2024).

[46] Turkish Statistical Institute-ABPRS (2022) Address Based Population Registration System.

[47] T. R. Ministry of Interior, SARS (2022) Spatial Address Registration System.

[48] T. R. Ministry of Environment, Urbanization and Climate Change.

[49] Turkish Statistical Institute (2021)-Building and Residence Characteristics Survey.

[50]Deierlein G, Reinhorn A, Willford M (2010) NEHRP seismic design technical brief no. 4—nonlinear structural analysis for seismic design: a guide for practicing engineers. In: NIST

INVESTIGATION ON STRUCTURAL DAMAGES OF RESIDENTAL RC BUILDINGS SUFFERED DUE TO KAHRAMANMARAŞ EARTHQUAKES

Editor

BETÜL ÜSTÜNER